KINETICS OF SILICA POLYMERIZATION AT VARIOUS CONDITIONS

A Thesis Submitted to
the Graduate School of Engineering and Sciences of
Izmir Institute of Technology
in Partial Fulfillment of the Requirements for the Degree of

MASTER OF SCIENCE

in Environmental Engineering

by
Öykü Çağ HASKÖYLÜ TOKER

March, 2022
İZMİR

ACKNOWLEDGEMENTS

This study was funded by the European Union's Horizon 2020 research and innovation program under grant agreement No. 850626 (REFLECT). I specially thank the European Union grant program for this support.

I would especially like to thank my supervisor, Prof. Dr. Mustafa M. Demir, for his guidance, support, encouragement, and insightful comments during the progress of my Master's thesis and the writing process. I would like to thank my co-supervisor, Prof. Dr. Alper Baba, for his contributions and support during my study. I would also like to thank the other members of the defense committee of my thesis, Assoc. Prof. Dr. Hatice Eser Ökten and Assist. Prof. Dr. Muhammed Üçüncü for their valuable suggestions and comments.

My special thanks to the Demir Lab research group members, Seyra Toprak, Berk Akgün, and Çağlar Erdem, for their support, friendship and help throughout my master's studies. I would also like to thank my friends Bora Okan and Gizem Taylan for their great support. A special thank you to Seyra Toprak who is not only a wonderful co-worker but also a sincere friend who shares our dreams and concerns.

Endless thanks to my dear family, my father and mother and my grandparents who always believed in me, supported and encouraged me. They have always been by my side and have been with me through this process.

Finally, a special thanks to my dear husband Fatih Toker who was always there for me, motivating me to do my best and comforting me in my stressful times.

ABSTRACT

KINETICS OF SILICA POLYMERIZATION AT VARIOUS CONDITIONS

Silica is the most abundant element on Earth because the Earth's crust is composed mainly of metal silicates. The source of this silica is mainly volcanic rocks, which come to the surface through tectonic activity and are the primary source of heat for geothermal activity. The silica concentration in a geothermal fluid is higher than the solubility limit of natural waters, so scaling of (metal) silicates is often observed in geothermal operations. This situation has become critical for geothermal power plants. Since silicates have an insulating structure, they lead to a reduction in energy efficiency during fluid transport. The formation of silica-rich deposits should be investigated to minimize the negative effects of the scaling. Briefly, silicic acid molecules in the reservoir system are condensed, and the monomeric silicic acid molecules bind to each other via covalent bonds. In the course of this reaction, dimers, tetramers and short oligomers are formed, and eventually a large polymeric silica network is formed. In the presence of metals, both the kinetics of polymerization and the structure of the network are inevitably affected. In this study, the presence of kinetic parameters (different salts such as $FeCl_3$, $MgCl_2$, $AlCl_3$ and NaCl), the reaction process, the rate, and the activation energy of silica polymerization at different temperatures between 25 and 90 °C were examined. The yellow silicomolybdate method was used to determine the concentration of monomeric silica. pH was found a stronger effect on the kinetics of silica polymerization than temperature. The neutral solution decreases rapidly, while the acidic solution has an induction phase in the first hour of polymerization. The order of the polymerization reaction was found as 3. The polymerization occurs in the initial phase, in the first 40 min, where the activation energy was found 29.52 ± 2.28 kJ/mol using Arrhenius equation and the rate constant was on the order of 4×10^{-8} $mol^{-2}\cdot L^{2}\cdot s^{-1}$.

ÖZET

ÇEŞİTLİ KOŞULLARDA SİLİCA POLİMERİZASYON KİNETİĞİ

Yer kabuğu başlıca metal silikatlardan oluştuğu için silika, dünyada en bol bulunan elementir. Bu silikanın kaynağı, esas olarak tektonik aktivitelerle yüzeye çıkan ve jeotermal aktivitenin ana ısı kaynağını oluşturan volkanik kayalardır. Jeotermal akışkanda silika konsantrasyonu doğal suların çözünürlük limitinden daha yüksektir, bu nedenle jeotermal işletmelerde (metal) silikatın kabuklaşması sıklıkla görülmektedir. Bu durum jeotermal enerji santralleri için kritik hale gelmiştir. Çünkü silikatlar yalıtkan bir yapıya sahip olup, akışkan taşınımı sırasında enerji verimliliğinin azaltılmasına neden olmaktadır. Sistemlerde oluşan bu kabuklanmanın olumsuz etkisini en aza indirmek için silika bakımından zengin bu tortunun oluşum mekanizmasının anlaşılması son derece önemlidir. Kısacası, sistemindeki silisik asit molekülleri yoğuşmaya uğramakta ve monomerik silisik asit molekülleri birbirine kovalent bağ ile bağlanmaktadır. Bu reaksiyon ilerledikçe dimerler, tetramerler ve kısa oligomerler oluşmakta ve sonunda büyük polimerik silika ağı gelişmektedir. Metallerin varlığında hem kinetik polimerizasyon hem de ağ yapısı kaçınılmaz olarak etkilenmektedir. Bu çalışma kapsamında, 25 ila 90 °C arasındaki çeşitli sıcaklıklarda silika polimerizasyonunun kinetik parametrelerinin ($FeCl_3$, $MgCl_2$, $AlCl_3$ ve NaCl gibi çeşitli tuzlar) varlığı, reaksiyon sırası, hızı ve aktivasyon enerjisi incelenmiştir. Monomerik silika konsantrasyonunun belirlenmesi için sarı silimolibdat yöntemi kullanılmıştır. Modellenmiş deneysel verilerin, üçüncü dereceden kinetik yasa tarafından takip ettiği belirlenmiştir. Bu, polimerizasyon mekanizmasının trimerler tarafından kontrol edildiği anlamına gelmektedir. Ancak, deneyler zaman aralıkları arasında incelenmiş ve bazı sonuçlar oran sıralamalarının üçüncü dereceden ikinci dereceye değiştirilebileceğini göstermiştir. Polimerizasyon başlangıç aşamasında, ilk 40 dakikada aktivasyon enerjisinin 29.52 ± 2.28 kJ/mol civarında ve hız sabitinin $4x10^{-8}$ $mol^{-2}\cdot L^{2}\cdot s^{-1}$ mertebesinde olduğu yerde gerçekleşmiştir. Sonuçlar ayrıca pH'ın silika polimerizasyonu kinetiği üzerinde sıcaklıktan daha güçlü bir etkiye sahip olduğu doğrulanmıştır. Nötr çözelti hızla azalırken, asidik çözelti polimerizasyonun ilk saatinde indüksiyon periyoduna sahiptir. Farklı sıcaklık, polimerizasyon hızını pH olarak etkilememiştir. 25°C'de deney en hızlı polimerizasyonu göstermiştir, ancak 90°C başlangıçtan itibaren düşük konsantrasyon değişikliği göstermiştir. Bütün bu deneyler sırasında, amorf silikanın kabuklaşması gözlemlenmezken, sadece silika polimerizasyonu gözlenmiştir.

TABLE OF CONTENTS

LIST OF FIGURES vii

LIST OF TABLES viii

CHAPTER 1. INTRODUCTION 1

CHAPTER 2. LITERATURE REVIEW 5

2.1. Silica and Its Formations 5

2.1.1. Silica in Natural Water Resources 6

2.2. Applications of Silica 7

2.3. Silica in Geothermal Brine 10

2.3.1. Silica Scaling in Geothermal Systems 11

2.4. Mechanism of Silica Polymerization 13

2.5. Parameters of Silica Polymerization 14

2.5.1. The effect of temperature 14

2.5.2. The effect of pH effect 15

2.5.3. The effect of ionic strength (salinity) 15

2.5.4. The effect of pressure 16

2.6. Monitoring the Silica Concentration 16

2.6.1. Spectrophotometry 16

2.6.2. Dynamic Light Scattering 16

2.6.3. Chromatography 16

2.6.4. Colorimetry – Silicomolybdate Method 17

2.7. Silica Removal 19

2.8. Kinetics of Silica Polymerization 20

CHAPTER 3. EXPERIMENTAL 21

3.1. Materials 21

3.2. Equipment 21

3.2.1 Spectroscopy 21

3.2.2. X-Ray Characterization Methods 22
3.2.3. Particle Characterization 22
3.3. Batch Experiment 23
3.3.1. Preparation of Silica Solution 24
3.3.2. Effect of Temperature 24
3.3.3. Effect of pH 24
3.3.4. Effect of Metal Ions 25
3.4. Batch Experiment with Tuzla Geothermal Brine 25
CHAPTER 4. RESULTS AND DISCUSSION 28
4.1. Silica Concentration 28
4.1.1. Determination of the concentration via spectroscopy 28
4.1.2. Effect of Temperature 30
4.1.3. Effect of Metal Ions 31
4.1.4 Effect of pH 34
4.1.5. Rate Order and Activation Energy 35
4.1.6 Experiments with Tuzla brine 40
CHAPTER 5. CONCLUSION 43
REFERENCES 44

LIST OF FIGURES

Figure **Page**

Figure 1.1. Location and geological map of the study area (Çanakkale, Ayvacık, Türkiye) 2

Figure 2. 1. Mineral composition of Earth's crust.....9

Figure 2. 2. Conceptual model of geothermal circulation, showing silicon cycling.....10

Figure 2. 3. Fe, Mg silicate deposit obtained from Tuzla Geothermal Power Plant. 11

Figure 2. 4. Tuzla Geothermal Power Plant located in Çanakkale, Ayvacık (Türkiye).....12

Figure 2. 5. Mechanism of particle growth. Part A represents the existing flocculating 13

Figure 3. 1. Schematic diagram of a UV-Spectrophotometer.....22

Figure 4. 1. Silicomolybdic samples from 20 mg/L to 100 mg/L.....28

Figure 4. 2. Calibration curve optical density at 434 nm and 452 nm wavelength.....29

Figure 4. 3. The concentration of dissolved silica at different temperatures at neutral pH. 30

Figure 4. 4. The concentration of dissolved silica. 31

Figure 4. 5. Silica concentration at 25 °C and 90 °C in the absence (blank) and with mixed metal ions. 33

Figure 4. 6. The concentration of monomeric silica at various pH.....34

Figure 4. 7. a) represent the separated part of the function utilized for the estimation of rate order: first 40 min and between 40-360 min b) an example of rate order calculation between time from 0 to 40 min for third order, $1/A^2$ (A represents the concentration of monomeric silica).....36

Figure 4. 8. Silica concentration at various pH for Tuzla geothermal brine. Dashed lines correspond to the solubility of amorphous silica at the 25 °C according to Dixit et al.....41

Figure 4. 9. Monomeric silica concentration at pH 5 and 9 at 90 °C for Tuzla geothermal brine. 41

Figure 4. 10. Monomeric silica concentration at 25°C and 90°C at neutral pH for Tuzla geothermal brine. 42

LIST OF TABLES

Table **Page**

Table 2. 1 Amount of soluble silica in water sources 5

Table 2. 2. Industries and products that commonly use amorphous silica 8

Table 2. 3. Percentage of scale content % p/p 12

Table 3. 1 Characteristics of Tuzla brine 26

Table 4. 1 Calibration curve at 434 nm and 452 nm wavelength. 29

Table 4. 2 Calculated concentration (mg/L) from the calibration curve 30

Table 4. 3. The rate constant of silica polymerization at different temperatures and neutral pH (without metals) 37

Table 4. 4. The rate constant of silica polymerization at 25 °C and 90 °C and neutral pH (with metals) 37

Table 4. 5. The rate constant of silica polymerization at 25 °C with various metal ions at neutral pH. 38

Table 4. 6. The activation energies of silica polymerization at different temperatures 39

Table 4. 7. The activation energies of silica polymerization at different temperatures 40

CHAPTER 1

INTRODUCTION

Silicates, one of the two main chemicals along with carbonates, are abundantly present in subsurface geothermal reservoirs. It is well established that silica scaling occurs when silica concentration in brine reaches supersaturation. Monomeric silica undergoes hydrolysis and condensation nucleate consecutively in three dimensions, forming polymeric networks. When the network reaches thermodynamically insoluble colloidal size, i.e. larger than the critical size of the nucleus, and deposit forms eventually as amorphous silica and/or metal silicates on surfaces of all types of equipment in power plants, for instance, heat exchangers, separators, vaporizer tubing, etc. Since silicates are insulator in nature, the formed deposits not only reduces energy harvesting of the power plant but also causes severe corrosion.[1] So that the formation of scaling forces to take a costly action. For example, cleaning the blockages in tubing leads to replacing pipes, drilling out clogged wells, causing environmental issues, and making re-injection wells tights. The solubility of silica and the polymerization rate are the two significant parameters to control this undesirable process.[2] Understanding the silica polymerization and polymerization kinetics rate may allow us to understand how fast the equilibrium is achieved, as a result of this a suitable action can be taken to mitigate this scaling.[3]

Silicate scaling has been heavily observed in the northern-west part of Türkiye. Tuzla geothermal power plant was selected as the main working field for our investigation. Because both amorphous and metal silicate scaling co-exists, heavy scaling is frequently observed in this system. Tuzla geothermal power plant is located in the northwestern part of Türkiye, 5 km from the Aegean Coast and 80 km south of Çanakkale. (Figure 1.1) It has been operated since January 2010.[4]

Tuzla geothermal plant has one re-injection well and three production wells with depths varying between 871 m and 539 m. The station has three production and two re-injection wells, and the energy production capacity is 7.5 Mwe.[1] Hot brine from the reservoir is not transferred straight to the turbine in the Tuzla geothermal plant's binary cycle geothermal power plant. Hot brine from the reservoir first enters the heat exchanger system, changing phases before entering the steam turbine.[5] Scaling made of silicate, which is the hardest to remove, is readily observed in the Tuzla geothermal system.[4]

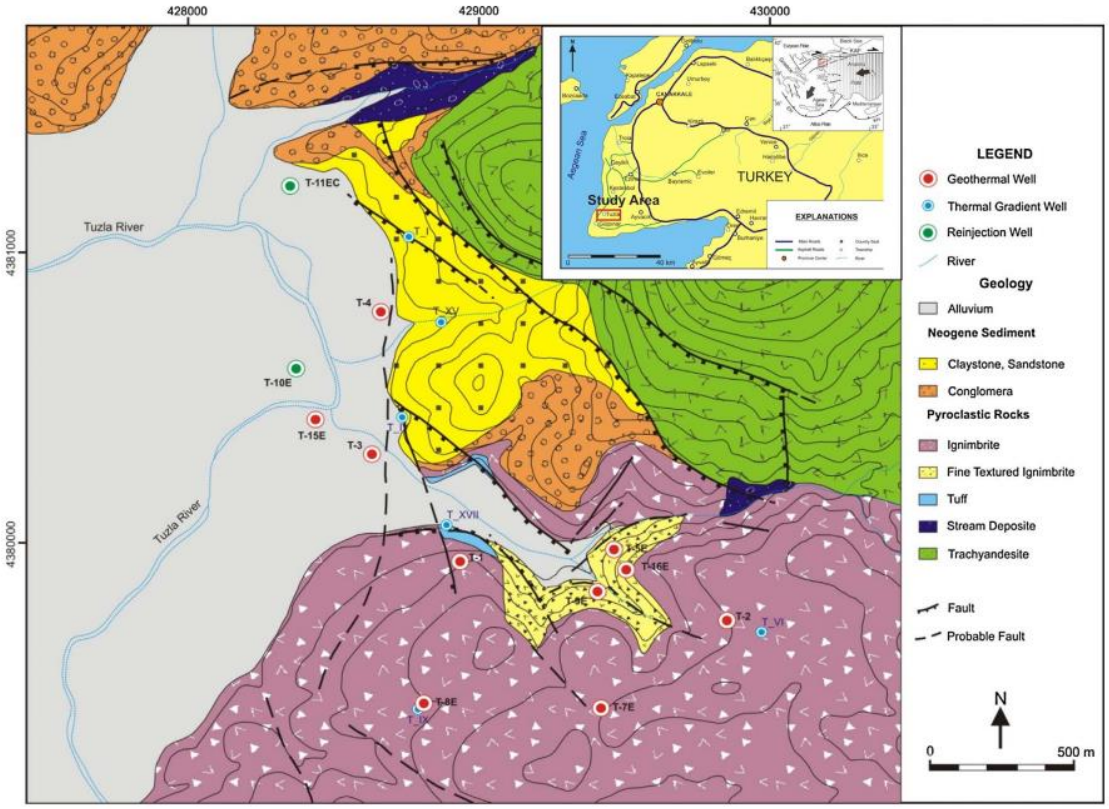

Figure 1.1. Location and geological map of the study area (Çanakkale, Ayvacık, Türkiye)

Tuzla Geothermal brine is found in a marble reservoir has been detected at a depth of 530 m and is located in a shallow volcanic pool at a depth of between 330 m to 550 m and is highly saline, containing 19,350 mg/L sodium and 36,380 mg/L chlorine concentration with a total hardness about 9000 ppm. [1,4] The electrical conductivity of the region is 83.4 mS/cm, which has two times higher salinity than seawater. The well-head temperature is 143 °C, and the re-injection temperature is nearly 104 °C. The composition of brine is rich in terms of almost all ions. Table 1 shows the ionic content of the brine obtained from the vaporizer. [1]

Table 1. The ionic content of the inlet brine was obtained from the vaporizer. [1]

pH	**EC (mS/cm)**	**T (°C)**	**P (bar)**	**Na (mg/L)**	**K (mg/L)**	**Mg (mg/L)**	**Ca (mg/L)**	**Cl (mg/L)**	**SO_4 (mg/L)**
7.65	91.9	142	3.1-3.5	19,330	1.93	119	3.05	35,960	183
HCO_3 (mg/L)	**SiO_2 (mg/L)**	**B (mg/L)**	**Ba (mg/L)**	**Cr (mg/L)**	**Fe (mg/L)**	**Li (mg/L)**	**Pb (mg/L)**	**Zn (mg/L)**	**Sr (mg/L)**
115	225	50.2	5.0	2.5	4.25	19.9	< 40	< 0.30	131.7

The concentrations of these minor components Sr, Cr, B, Ba, Li and range from 131.7 to 175.8 mg/L; from 19.9 to 25.6; from 50.2 to 75.1; from 5.0 to 6.0; from 0.5 to 3.2; from <0.30 to 0.65; and, respectively of the geothermal brines. B and Sr concentrations in geothermal fluids are incredibly high in the Tuzla geothermal field. The degassing of magma intrusive may also control this issue related to volcanic rocks. Additionally, Tuzla brine contains 195-225 mg/L of silica (SiO_2). Under high pressure and high-temperature conditions, quartz is soluble in the brine in the reservoir.[6]

The dissolution of ferromangnesium minerals within Miocene volcanic rocks, composed of trachyte, andesite, and trachyteandesite, is the cause of the geothermal brine's dark and reddish colors and high Mg and Fe concentrations. Among the highly changed sedimentary rocks are quartz, K-feldspar, biotite, amphibole, sanidine, chalcopyrite, pyrite, and hematite.[7]

At the Tuzla geothermal binary plant, scale formation, in addition to reducing the amount of brine flow going through the vaporizer, vaporizer tubes also reduce the heat transfer from the brine to the motive fluid, *n*-pentane, which lowers the power plant's energy production. As the scale analysis indicates, silica, magnesium, and iron constitute most of the scale's composition. (Table 2.3)

The equilibrium chemistry of the brine is the crucial parameter for understanding kinetics. It is claimed that polymerization starts when the concentration of monomeric silica reaches the solubility of amorphous silica.[3] Rates of silica polymerization roughly followed the Arrhenius equation at relatively low temperatures between 20 and 60°C.[8, 9, 10, 11]

When dissolved silica concentrations in aqueous solutions are high enough, the excess silica can be converted into colloidal amorphous silica via two different mechanisms. The first mechanism is the formation of a silica network; the second is the formation of colloidal particles from the nucleation of an amorphous silica phase; and the last one is the growth of the amorphous silica particles via aggregation of individual small colloids. [12]

This thesis investigated the kinetics of silica polymerization concerning pH, temperature, chemistry, and concentration of existing metal ions using both synthetic solution and neutral brine obtained from the Tuzla region. The polymerization mechanism of the silica experiment was performed with the following monomeric silica concentration by preparing silica solution with the initial concentration of 0.01 M. Yellow silicomolybdate method, which is known easy applicable and fast-resulting way, was used to figure out the polymerization mechanism by measuring UV-VIS spectrophotometer. Based on

spectrometric results, the Arrhenius type of equation is applied to determine the activation energy of the polymerization under different conditions.

CHAPTER 2

LITERATURE REVIEW

2.1. Silica and Its Formations

Most of the earth's crust is made up of silica, yet there is still much to learn about its chemistry, particularly how it behaves in terms of solubility in water.[13] From the aspect of scaling, Silica, one of the most abundant natural compounds, has a presence of 12% in the Earth's crust, surface soils, and all major rock types with its crystalline forms. [14] However, several different types of silica exist, including quartz, tridymite, cristobalite, amorphous silica, and others.[3]

Despite its stable structure as quartz, silica is continuously dissolved and precipitated over a significant portion of the earth's surface.[13]

Table 2. 1 Amount of soluble silica in water sources[13]

Source of silica	**Range in ppm as SiO_2**
River waters	5 to 35, a few up to 75
Seawater	5 to 15
Surface water (Pacific Ocean)	0.0001-0.3

As can be seen from Table 2.1, silicates typically range from 20 to 60 parts per million (ppm) in natural water, although they can reach 100 ppm. Furthermore, silica's fundamental chemistry is quite complex due to the variety of species in the aqueous solution that change with pH, ionic strength, and temperature.[13]

Since the 1950s, various amorphous silicas have been commercially available and utilized in multiple industrial applications and goods.[15] White powders or white dispersions of these powders are the typical forms of synthetic amorphous silica. Although they are hydrophilic, surface modification makes it simple to make them hydrophobic. They can be made as silica gels, precipitated silica, or fumed silica. One of the processes involves adding acid to an alkali metal silicate solution to create a gelatinous precipitate. This residue is then

washed and dried to fabricate colorless microporous silica particles. The physical-chemical characteristics of the product can be manipulated by changing things like the flame temperature, flame composition, and feedstock.[16] Fumed and precipitated silica, silica gel, and colloidal amorphous silica are the four main types of synthetic amorphous silica.[17]

When the temperature is ambient, monosilicic acid condenses to generate disilicic acid, followed by adding monomers to form trisilicic acid and tetrasilicic acid.[18]

2.1.1. Silica in Natural Water Resources

In an aqueous solution, silica exists in several different forms, and the silicate ion will exist in a solution together with $Si(OH)_4$ concerning the following reaction:

$$Si(OH)_4 + (OH)^- \rightarrow SiO(OH)_3^- + H_2O$$

When the concentration of SiO_2 is found to be about 110 – 140 ppm

In the pH range of 1-8, monomeric silica $Si(OH)_4$ is the solution's stable form. When the pH is increased to 9, the amorphous silica solubility rises sharply to the formation of silicate ions concerning shown reaction above.[19]

Water-rock interaction is the only source of silica in groundwater. The silica formed by the chemical weathering of silicate minerals in rocks and sediments is dissolved by the constantly flowing groundwater. It is known that the deeper reservoir water contains more silica than shallow groundwater. [20]

$Si(OH)_4 + Si(OH)_4 \rightarrow {}_3(HO)\text{-}Si\text{-}O\text{-}Si\text{-}(OH)_3 \rightarrow$ Oligomers $\rightarrow (SiO_2)_n$ (silica polymer)

$Si(OH)_4 + Al(OH)_3 \rightarrow {}_3(HO)\text{-}Si\text{-}O\text{-}Al(OH)_2 \rightarrow {}_3(HO)\text{-}Si\text{-}Al(OH)\text{-}O\text{-}Si(OH)_3 \rightarrow$ (Al silicate)

$Si(OH)_4 + Fe(OH)_3 \rightarrow {}_3(HO)\text{-}Si\text{-}O\text{-}Fe(OH)_2 \rightarrow {}_3(HO)\text{-}Si\text{-}O\text{-}Fe(OH)\text{-}O\text{-}Si(OH)_3 \rightarrow$ (Fe silicate)

$Si(OH)_4 + Mg(OH)_3 \rightarrow {}_3(HO)\text{-}Si\text{-}O\text{-}Mg\text{-}OH \rightarrow {}_3(HO)\text{-}Si\text{-}O\text{-}Mg\text{-}O\text{-}Si(OH)_3 \rightarrow$ (Mg silicate)

$Si(OH)_4 + Ca(OH)_2 \rightarrow {}_3(HO)\text{-}Si\text{-}O\text{-}Ca\text{-}OH \rightarrow {}_3(HO)\text{-}Si\text{-}O\text{-}Ca\text{-}O\text{-}Si(OH)_3 \rightarrow$ (Ca silicate) [21]

2.2. Applications of Silica

Amorphous silica particles suspended in a liquid are called colloidal silica. To keep the colloids suspended in the solution, the colloids need to be either sterically or electrostatically stabilized. All the available colloidal silica grades are made up of silica particles that are either perfectly spherical or slightly irregular in shape and range in size from roughly nanometer to submicrometer in diameter. According to the colloidal silica's particle size, dispersions with small particles (10 nm) are typically relatively straightforward, those with medium-sized particles (10–20 nm) tend to seem opalescent, and those with large particles (>50 nm) are typically colorless.[22] Rayleigh scattering may be the main issue in the appearance of the dispersions.

To reinforce elastomer products like tires, shoe bottoms, and mechanical rubber products, precipitated silica is generated in large amounts. Primary particles in the precipitated silica are typically in the 5-100 nm range and form tightly bound aggregates in the 0.1-mm range.

Following precipitation, silica can be filtered using various methods, including belt filters, membrane filters, and filter presses. To get the proper particle size distribution, it is frequently washed to remove salts and dried before milling, which is the last step in the manufacturing process. A trace quantity of metal oxides, sulfates, or chlorides may be present in the precipitated silica's end product, which typically has a purity of about 95% [15]

Sand and gravel, often used for industrial applications, are called silica sand, silica, and quartz sand due to their high silicon dioxide (SiO_2) content. Since silica is a natural formation on the Earth, even if the specifications for each application area vary, the resources of silica are abundant. Scope of the environment, silica mining does not cause a problem. Table 2.2 summarizes the applications of silica in a wide range of industrial fields.

Table 2. 2. Industries and products that commonly use amorphous silica [22]

Application	Silica Use
Adhesives	Adding to aqueous adhesive compositions improves the mechanical and thermal stability of bonded connections. It reduces the time needed for dry organic dispersions and helps modify viscosity.
Cosmetics	Used to offer a smooth feel to foundations and cosmetics and help minimize skin shine, oil and perspiration absorption, and sebum production.
Concrete	Functions as a stabilizer, durability booster, speed-up, and strength builder.
Dentals	Silica gel imparts no taste, has a low refractive index for good clarity, and offers stability for prolonged shelf life.
Food Industry	Used as a practical processing aid to get rid of undesirable elements from liquids, it allows the changing of viscosity.
Ground consolidation	Ensures the surface is impervious to liquids such as water or other waterborne chemicals.
Paints and coatings	Increases the hardness of decorative coatings, improves pigment dispersion, and extends their opening time.
Paper manufacturing	Used to improve the printing and gliding characteristics of board stock. Usual retention and drainage aids for papermaking. can be used to make an anti-slip surface on paper and packaging materials.
Pharmaceutical	May be used to absorb moisture, stop caking, let the powder flow easier, reduce sticking, and give items a longer shelf life.
Plastic Films	Enhances the films' anti-blocking capabilities

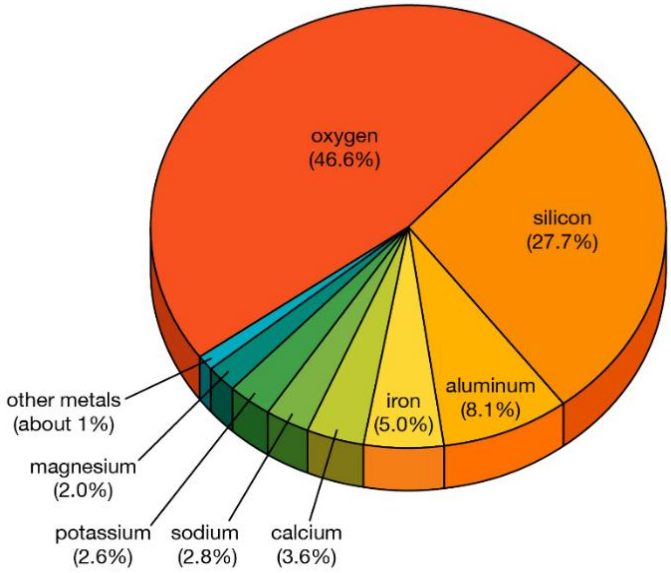

Figure 2. 1. Mineral composition of Earth's crust

Silica is a crucial sorbent when separating a wide range of organic chemicals using column and thin-layer chromatography. It is used to purify organic molecules such as lipids, steroids, fat-soluble vitamins, and natural products in commercial and research labs. Additionally, chromatographic techniques are utilized to isolate specific chemical components from mixtures. [14]

Fig 2.1 shows the mineral composition of Earth's crust. It is clearly shows silica abundance in the crust. According to reports, soluble silica can react with and precipitate amorphous hydroxides of AI, Fe, Mn, or Mg, bringing the concentration down to as low as 3 ppm. [3]

2.3. Silica in Geothermal Brine

According to geological evidence, the equilibrium solubility of quartz in hot reservoirs determines the silica concentration. To release its stored thermal energy, the hot brine is flashed or cooled as it moves through a power plant system after being brought to the surface.[3] (Fig 2.2) Fluid management becomes challenging as the fluids cool because they frequently become supersaturated with secondary minerals. [3,23,24]

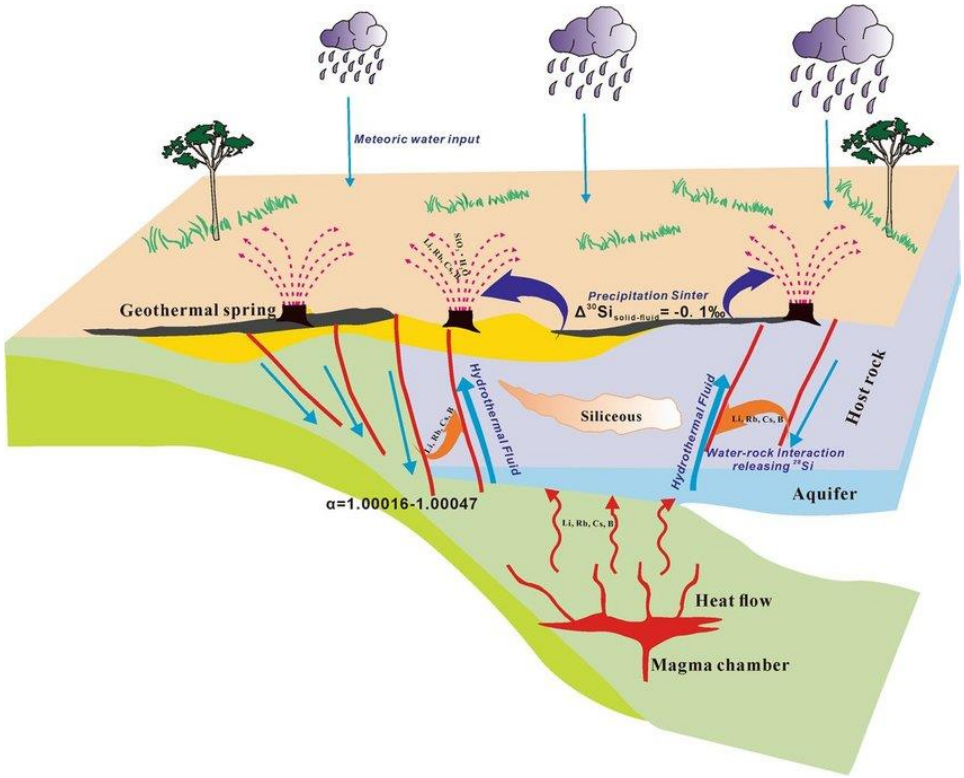

Figure 2. 2. Conceptual model of geothermal circulation, showing silicon cycling [25]

When silica reaches the surface, the silica is concentrated in the fluid. The separation occurred between steam and water because the temperature and pressure decreased. As a result of this sudden change, silica becomes oversaturated, and scale formation is observed, which is the most problematic situation for geothermal power plants. Many methods have been proposed to prevent silica scalings, such as pH modification, inhibitors, or controlled precipitation using silica gel. Other methods like these can provide efficient results for the applied geothermal power plant. However, it is not possible to talk about a single universal way to prevent silica scaling. [23]

2.3.1. Silica Scaling in Geothermal Systems

Many methods have been proposed so far to minimize the scaling of silica. Controlled precipitation by the addition of silica gel adding organic antiscalants, [26] mixing the wastewater with low silica concentration,[27] increasing or decreasing the pH of the wastewater,[28, 29] cationic reactants to trigger silica deposition [30], storage in a retention pond [31] are some of these methods. Even though these techniques have been proven effective in geothermal sites, no all-encompassing approach to stop silica scaling has been created.

Figure 2. 3. Fe, Mg silicate deposit obtained from Tuzla Geothermal Power Plant.

2.3.1.1. Silica in Tuzla Geothermal Brine Water

The Tuzla Geothermal Power Plant is situated in Çanakkale, northwest of Türkiye.(Fig 2.4) The brine and steam components of the two-phase geothermal fluid produced by artesian flow from two production wells are separated at the well-head horizontal separators, and the brine is transferred to the ORC (Organic Rankine Cycle) Plant by booster pumps. In contrast, the steam arrives at the plant naturally.

Figure 2. 4. Tuzla Geothermal Power Plant located in Çanakkale, Ayvacık (Türkiye)

Although the brine water has a hardness of about 9 g/L, the calcium carbonate scale can be prevented successfully using phosphate and phosphonate containing antiscalants. Yet, the silica scaling has not been stopped since the chemistry is more complex.[1] Metal silicate formation has occurred in the preheater and vaporizer parts called heat exchangers and separated brine lines. The scale deposition at the vaporizer tubes reduces the heat transfer from the brine to the motive fluid n-pentane and reduces the volume of brine flows through the vaporizer, reducing the power plant's energy output. Scale analysis shows the content of the scale is mainly iron, silica, and magnesium. Figure 2.3 shows Mg-Fe silicate deposit in Tuzla area. Scale samples analysis shows iron, magnesium, oxygen, calcium, manganese, silicon, and iron all contribute to the various layers of the modification.[4]

Table 2. 3. Percentage of scale content [4] % p/p

Element	**U.M.**	**Value**
Magnesium	MgO	14.4
Silicon	SiO_2	50.4
Calcium	CaO	1.58
Iron	Fe_2O_3	22.7
Chlorine	Cl	2.3
Aluminium	Al_3O_3	0.39
Phosphor	P_2O_5	0.13
Sulfur	SO3	0.21
Zinc	ZnO	0.57

2.4. Mechanism of Silica Polymerization

The basic definition of silica polymerization is forming a sizeable molecular network from a low-molecular-weight silica precursor. These molecules are called 'monomers.' Silica polymerization occurs when the amount of monosilicic acid ($Si(OH)_4$) in an aqueous solution exceeds the amount of amorphous silica. As the polymerization progress, an excess amount of monomers in the solution progressively disappear.[2] Eventually, silica gels or powders are obtained, as represented in Figure 2.5.[13] Polymerization of two $Si(OH)_4$ begins when the solution is concentrated, and a solution contains higher than only 140 ppm as SiO_2 can be enough to follow the polymerization mechanism. Then, the silicic acid ($Si(OH)_4$) tends to rise to polysilicic acid resulting in a colloid, gel, or precipitate. This polymerization starts with the formation of disilicic acid. It continues with the appearance of trisilicic acid, and the increased size of this species forms colloidal particles or, if the condition is suitable, a gel. [19]

Geothermal power plant pipes and water heater scaling, catalytic and ceramic applications, and coating applications to increase adhesion and wetting properties extensively appear for broad industrial and environmental processes for silica polymerization and silica precipitation. [32]

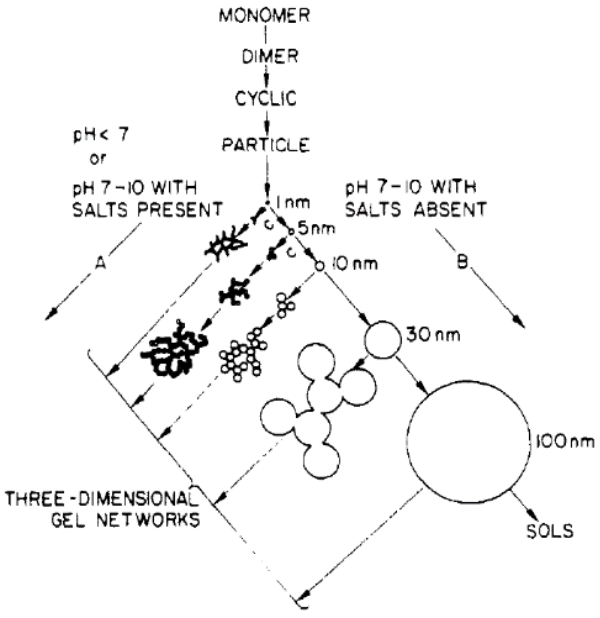

Figure 2. 5. Mechanism of particle growth. Part A represents the existing flocculating salts or acid solutions. Part B describes the particles in sol increase in size as they get smaller. [13]

As the product of the polymerization reaction, the nano-colloid or bigger forms of silica can cause clogging and scaling problems, it should be kept under control by tunning conditions of polymerization. Many studies show that silica polymerization is highly dependent on pH and temperature. However, the effect of salinity, existing ions, ionic strength, flow rates, aeration, and degree of supersaturation are also examined by many authors since all of them affect the polymerization behavior. [18,32-33]

2.5. Parameters of Silica Polymerization

The elemental composition of the solution, its level of supersaturation concerning amorphous silica, its pH and temperature, and its ionic strength are the primary factors affecting the reaction of silica polymerization and precipitation, according to previous studies on silica precipitation. [12,34,23] Similar observations on the precipitation of amorphous silica have been reported [4,28,35–39], despite some differences between these research, specifically on the kinetic law employed to predict the precipitation rate or on the impact of ph. For example, as a common fact about precipitation, amorphous silica precipitation is proportional to the ionic strength (salinity) and the degree of supersaturation of fluid. However, it is inversely proportional to temperature. [40]

2.5.1. The effect of temperature

Since the silica scaling occurs mainly in high-chloride and hot water systems similar to geothermal brine, have recently drawn interest. This issue has intensified the studies to understand temperature's effect on silica and show how the polymerization mechanism changes.

The reactions exhibit induction periods, whose durations change with temperature and become shorter as the supersaturation concentration increases. It is known that the reaction rate is mostly not affected by temperature since smaller but larger polymers form at higher temperatures. Rothbaum et al. showed that the total silica concentration remains unchanged when temperature changes, but the shape of the silica molecules changes throughout polymerization at between 5 °C to 90 °C. However, it is found that when the temperature increases from 90 °C, silica precipitation occurs because of the formation of an extensive silica molecular network. [41]

Although various studies have examined the temperature effect on silica polymerization, the results were inconsistent. On the other hand, the induction period was also observed inconstantly. It was stated that this situation may be related to the starting silica material used in the study, the concentration of this material, and whether it is synthetic or geothermal brine. However, the typical result was temperature has a lower effect on silica polymerization among other parameters such as pH, salinity, and supersaturation.

2.5.2. The effect of pH effect

Silica polymerization is known to be highly dependent on the pH of the solution. Comparing the temperature and pH dependence of polymerization, Dixit et. al. Icopini et. al., and Choppin et. al. reported that pH has more effect on polymerization than temperature. [14,35,42] This strong dependence on pH is seen by catalyzing with a hydroxyl ion of polymerization in a neutral or alkaline medium.

On the other hand, at higher pH, the silicic acids seem to be made up of monomers and much larger molecular weight polysilicic acids, or at least species that do not readily react with molybdic acid. When the alkalinity of the solution increases (i.e., > 9), the reaction rate decreases.

2.5.3. The effect of ionic strength (salinity)

The salinity effect on silica polymerization showed that the solubility of amorphous silica was not significantly affected by the somewhat low concentration dissolved salts.[2] On the other hand, other studies show that amorphous silica solubility is highly dependent on the presence of salt. For example, amorphous silica solubility was found at 77.7 ppm in 1 M $NaClO_4$ solution at 25 °C while between 100-120 ppm in neutral water without salt.[2,43,35] Also, the effect of the addition or presence of aluminum remarkably decreased the solubility. Since polymerization is directly related to the solubility of amorphous silica and how salinity affects solubility, it is valid for polymerization. [10,13]

2.5.4. The effect of pressure

Some studies showed that silica solubility is proportional to pressure. It was reported as when the pressure increased from 1 to 150 atm. The solubility increased from 65 to 71 ppm. At pressures up to a few hundred bars and temperatures below 100°C, it has been demonstrated that the effects of pressure on silica solubility are minimal. [44,45] The general decision about pressure effect on polymerization is less significant than pH and temperature. [2]

2.6. Monitoring the Silica Concentration

The most frequently employed methods include spectrophotometry, chromatography, and light scattering.

2.6.1. Spectrophotometry

Silica directly interferes with spectrophotometric measurements at particular light spectrum wavelengths. [46] Spectrophotometry helps to determine the concentration of the dissolved silica in natural water and the absorbance of colored species such as yellow or blue molybdosilicic acid. The silicomolybdate method will be explained detailed in Section 2.6. [Kent Fanning]

2.6.2. Dynamic Light Scattering

An examination of the time-resolved degradation of the concentration of monomeric silica using the silicomolybdate method can be given with the light scattering experiments (DLS). DLS study shows the assessment of particle size of the SiO_2 particles. [33]

2.6.3. Chromatography

To use the chromatographic method, first, the detected type of silica should be determined. Ion chromatography can also measure the dissolved silica mentioned in this

thesis. When silica occurs as the anion of a weak acid, it can be retained poorly by anion exchange columns. Also, low concentrations of silicon and other ions, such as phosphorus and arsenic, are determined spectrophotometrically with hetero-poly compounds. However, the determination of each of them is not easy due to their similar interaction with hetero-poly compounds and the similar physicochemical properties for the spectrophotometric method.

In conjunction with spectrophotometric detection, high-performance liquid chromatography (HPLC) enables the simultaneous separation and determination of all sample components. It is possible to increase the selectivity of hetero-element resolution when they co-exist.

2.6.4. Colorimetry – Silicomolybdate Method

The amount of dissolved silica in natural water is generally measured by the absorbance of colored species of molybdosilicic acid ($H_4SiMo_{12}O_{10}$). All methods for the analysis require the manufacture of an unreduced form of this heteropoly acid.[47] The depletion of silicic acid during the polymerization process can be determined by the silicomolybdate method.[33]

Silicomolybdic acid has two isomers: α (alpha) and β (beta) silicomolybdate. The difference between these two forms of silicomolybdate is pH when these molecules are dissolved in the aqueous medium.[48] The development of a yellow molybdosilicate acid complex, which has two forms depending on the pH, is the foundation of traditional methods for measuring dissolved silicate. [49]

2.6.4.1. α and β – Silicomolybdate

Unreduced *β*-silicomolybdic acid has a greater absorbance than *α*- silicomolybdic acid from 335-500 nm. Also, β-silicomolybdic acid has an absorbance peak more significant than any absorbance peak of the reduced α-isomer. Thus, because of its sensitivity, *β*-isomer silicomolybdic acid is preferred for many analytical methods.

2.6.4.2. Blue Silicomolybdic Acid Method

The blue silicomolybdic method relies on the reaction of silicic acid with acidified ammonium heptamolybdate. This method is more suitable for containing a low silica concentration because the absorbance of the blue species is higher than that of the yellow species. [33] The significantly higher absorbance increases sensitivity potentially tenfold if the yellow complex is converted to molybdenum blue and a reagent is applied that will not remove the remaining excess of molybdic acid. Developing the color in the perchloric acid medium through reduction with stannous ion and ascorbic acid, which removes interferences and produces a stable color, is another modification of the molybdenum blue process. [50]

2.6.4.3. Yellow Silicomolybdic Acid Method

The reaction of molybdic acid with monomeric $Si(OH)_4$ yields yellow silicomolybdic acid. Since the last molecule contains only one silicon atom, it is evident that only $Si(OH)_4$, and not polymers of it, may directly react with acidified ammonium heptamolybdate to generate the yellow silicomolybdic acid. Since ammonium molybdate has a molecular weight of 1235.9, 35.3 g of ammonium molybdate is consumed by 1 g of silica. [13]

$$7Si(OH)_4 + 12H_6Mo_7O_{24}\cdot 4H_2O + 17H_2O \Leftrightarrow 7H_4SiMo_{12}O_{40}\cdot 29H_2O$$

In this method, when polymers are present, polysilicic acid depolymerizes slowly enough that the monomer can be identified by observing how quickly the color changes. [13]

The yellow silicomolybdate method is different from than blue silicomolybdate method with its absorbance. While the addition of acidified ammonium molybdate and acid between 0 to 1000 mg/L SiO_2-containing solution is measured at a wavelength between 370 to 470 nm.

2.7. Silica Removal

Since the silica scaling problem increases maintenance and repair costs and decreases system efficiency, it is tried to be controlled or even stopped. In some systems, solutions are applied only for the scaling problem without preventing the presence of silica. In contrast, in others, it is aimed to reduce the amount of silica as much as possible.

For example, coagulation is offered as an effective alternative to reduce the silica content in waste from recycled paper mills. The coagulation process was carried out using various poly-aluminum chlorides (PACls) or $FeCl_3$ in waters intended to be recycled with a final reverse osmosis (RO) step. At pH 10.5, PACls with low alumina concentration and strong basicity removed silica almost entirely. By adding one of these PACls, a sound reduction in the silica level was achieved without altering the pH. [51]

Considering the drinking water treatment, because there are no bivalent cations present in the feed water, some fouling or scaling problems occur because of silica and silica-derived precipitants at high-recovery reverse osmosis systems. Between testing, the precipitation of silica with $Al(OH)_3$, $Fe(OH)_3$, and silica gel was investigated, and the removal of silica using a strongly basic anion (SBA) exchange resin $Al(OH)_3$ was found as the most effective precipitant for silica removing. This has provided nearly all the molecularly dissolved silica with a 94% removal yield. [52]

Similarly, three sparingly soluble magnesium compounds ($Mg(OH)_2{\cdot}5H_2O$, $Mg(CO_3)_4$, $Mg(OH)_2$, and MgO were investigated for silica removal from drinking water treatment processes at various pH and various dosages of Mg. Since the silica removal rate remained at 40%, some preliminary activities were applied as it was insufficient to eliminate the scaling problem. When slurries of poorly soluble compounds were tested under the same conditions after pre-acidification with concentrated sulfuric acid, it was observed that the removal efficiency was increased up to 86% at pH 11.5. As a result of this test, it has ensured that it is used in the reverse osmosis system used in the drinking water treatment system, with an efficiency of about 80%, without the formation of silica scaling. [53]

Another membrane system with silica scaling is a significant challenge in desalination, especially for the internal desalination of geothermal brine or brackish groundwater, which often contains high concentrations of silica and dissolved solids. Membrane distillation (MD) was used as a thermally driven membrane desalination

technique that is not limited to the increased osmotic pressure of the feed as in a reverse osmosis system.

2.8. Kinetics of Silica Polymerization

The formation of high-molecular particles from low-molecular particles is called polymerization. Chemical kinetics is the definition of the rate of a chemical reaction, and it is used to understand the chemical conversion between reactants and products. Since a rate is a change in the quantity that occurs with time, we are most concerned with the change in silica concentration. Both temperature and pressure drop significantly as the geothermal fluid rises the well and reaches the surface of the power plant. Since the silica solubility is controlled by amorphous silica in geothermal brines, the conversion between monomeric silica and amorphous silica should be considered. [10,31,54]

Silica kinetics are essential in thermally enhanced oil recovery and remediation of subsurface pollution, reactive waste disposal by burial, and geothermal runoff by subsurface injection. [38]

To understand the kinetics of silica polymerization, the reaction rate needs to be considered. Therefore, pH, temperature, pressure, and salinity affect polymerization kinetics. [42] In this thesis, the kinetics of silica polymerization was monitored by considering the pH and temperature parameters. The rate constants were calculated according to the temperature parameter, and how the polymerization mechanism worked was observed.

CHAPTER 3

EXPERIMENTAL

3.1. Materials

Experiments were conducted with both synthetic silica solution and geothermal brine. Sodium silicate solution (extra pure) was supplied from Merck (Darmstadt, Germany). Ammonium Heptamolybdate (cryst. extra pure) was supplied from Merck (Darmstadt, Germany) for the colorimetric method measurement. For pH adjustment, Sulfuric acid (H_2SO_4) ACS reagent 95-97% was supplied from ISOLAB (Wertheim, Germany), and Sodium Hydroxide (NaOH) (pellets, purest grade) was provided by Sigma-Aldrich (St. Louis, MO, USA). For the existence of metal ions experiment Magnesium Chloride ($MgCl_2$), Aluminum Chloride ($AlCl_3$) anhydrous powder of 99.9% trace metal basis, Iron (III) Chloride ($FeCl_3$) powder, Sodium Chloride (NaCl) of 99% purity, were supplied Sigma-Aldrich (St. Louis, MO, USA).

3.2. Equipment

3.2.1 Spectroscopy

The concentration of monomeric silica was monitored spectrophotometrically. The molybdate yellow method was used as the colorimetric measurement by analyzing HACH UV-spectrophotometer (Düsseldorf, Germany). The device has an automatic measurement program for low and high silica concentrations and the wavelength scanning mode. A spectrophotometry technique uses light intensity measurements as a beam of light travels through a sample solution to determine how much a chemical compound absorbs light. The fundamental idea is that every substance has a specific range of wavelengths within which it either absorbs or transmits light. The measurement procedure presented in Fig 3.1.

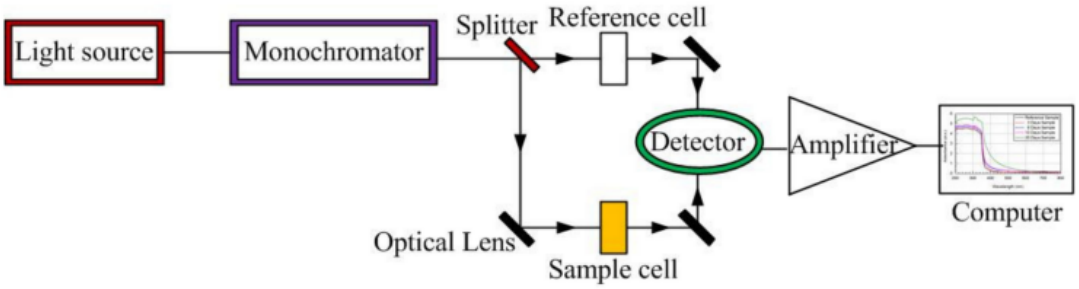

Figure 3. 1. Schematic diagram of a UV-Spectrophotometer [55]

The wavelength scanning mode was adjusted from 350 to 600 nm. Since the automatic measurement shows SiO_2 concentration at 452 nm, the intensity results from wavelength scanning were recorded at 452 nm and 434 nm to check the precision. To calculate unknown SiO_2 concentration, this calibration curve was prepared with a standard HACH stock solution containing 1000 ppm SiO_2.

3.2.2. X-Ray Characterization Methods

X-Ray fluorescence (XRF) spectroscopy (SPECTRO IQ II (Kleve, Germany) analysis was done to characterize the elemental composition of the solution and the precipitated formation. An X-ray diffractometer (XRD), Philips X'Pert Pro Eindhoven, Netherlands) was used to obtain the silica formation's dried and precipitated crystalline structure. A copper anode was used as the X-ray source, along with a generator voltage of 45 kV, a Cu-Kα wavelength of 1.5406 Å, and a tube current of 40 mA. The sample was scanned at the rate of 0.08° per second and scanned between the 2θ angles of 10° - 80°.

3.2.3. Particle Characterization

Scanning Electron Microscopy (SEM), FEI Quanta 250 Feg (Oregon, USA), was used to analyze the dried or precipitated silica morphology. Malvern dynamic light scattering (DLS) Nano-ZS instrument (Worcestershire, UK) was used to determine the colloids' particle size, distribution, and zeta potential.

3.3. Batch Experiment

Several batch experiments were performed to understand the polymerization mechanism of silica. First, a synthetic SiO_2 dispersion was prepared by diluting with sodium silicate solution in deionized water containing 1000 ppm SiO_2. All experiment parts were performed in polypropylene beakers to prevent possible silica interference. After the synthetic solution was prepared, after only 5 min, the first sample was taken and recorded as the initial concentration of the solution. The concentration of the artificial solution was calculated based on the HACH standard solution's calibration values to ensure the measurement's accuracy. The spectrophotometric silica molybdate yellow method measured the dissolved (monomeric) silica species. After the sample was taken, ammonium molybdate and sulfuric acid were added to the sample taken to be able to measure the spectrophotometer. The remaining part of the solution, after 6 h-experiment, was placed in an oven, and the precipitated part was taken for analysis.

Each absorbance of the samples was recorded to identify the change in the concentration of monomeric silica from the calibrated values. According to these results, the rate of the experiment was calculated by Equation (3.1) and integrated into Arrhenius Equation as shown in Equation (3.2)

$$\text{rate}=k\,[A]^a\,[B]^b \tag{3.1}$$

Where k is the rate constant; A is the concentration in ($mol \cdot L^{-1}$); B is the concentration ($mol \cdot L^{-1}$); a is the order of reaction concerning A; b is the reaction relating to B.

$$k = Ae^{(-E_a)/RT} \tag{3.2}$$

k is the rate constant; E_a is the activation energy ($J \cdot mol^{-1}$); T is the temperature in K; R is the gas constant ($J \cdot mol^{-1}\,K^{-1}$); A is the pre-exponential factor; e is the base of the natural logarithm.

The pH of the prepared silica solution was detected as 10.1, so it was adjusted to the desired pH of 5, 7, and 9 to understand the polymerization behavior concerning pH. Then,

the same experiments were performed at different temperatures as 25 °C, 45 °C, and 90 °C, to achieve enough data for the kinetic computations.

3.3.1. Preparation of Silica Solution

Synthetic silica solution was prepared to contain 1000 ppm SiO_2, diluting $Na_2SiO_2 \cdot 2H_2O$ solution in 250 mL of deionized water. The first sample was taken as soon as possible to detect the initial concentration before the polymerization began.

Therefore, after sampling, 500 µL ammonium molybdate and 500 µL sulfuric acid were added to earn the yellow color showing the SiO_2 concentration. 100 gL^{-1} ammonium molybdate solution was prepared by dissolving 5 g of ammonium heptamolybdate in 100 mL deionized water. For the preparation of 1.5 M of H_2SO_4, which was to make acidified media for the silicomolybdate in the experiments, 20,8 mL of 98% H_2SO_4 (18 M) was taken, first added to 250 mL deionized water in a 500 mL volumetric flask, and then completed with deionized water up to 500 mL. For the 500 mL volumetric flask used to prepare the 1M of HCl to adjust the pH, 41.6 mL of 37% HCl (12 M) was taken and poured into 250 mL of deionized water first.

3.3.2. Effect of Temperature

To find out the effect of temperature on silica polymerization, experiments were performed at room temperature, 25 °C (298 K), 45 °C (318 K), and 90 °C (363 K). Beakers were placed into the water bath to keep the temperature constant.

3.3.3. Effect of pH

To find out the effect of the solution on silica polymerization with different pH values as 5, 7, and 9, and stirred continuously at room temperature for 6h. 1.5 M HCl and 1.5 M of NaOH were added to solutions by using droplets.

3.3.4. Effect of Metal Ions

The experiment aimed to understand how metal ions affect silica scaling. It is well established that silica scaling occurs by iron or manganese salts. Therefore, existing metal ions in geothermal brine may accelerate or inhibit silica polymerization. [56,57]

$FeCl_3$, $AlCl_3$, $MgCl_2$, and NaCl were added separately to the sodium silicate solution to determine the effect of metals on the silica polymerization. When the concentration of silicate solution is 0.01 M, the concentration of salts was found to be 2×10^{-4} M. The solutions to the effect of Fe^{3+}, Al^{3+}, $Mg2^{+}$, and Na^{+} on silica polymerization were prepared by dissolving 32.4 mg of $FeCl_3$, 19 mg of $MgCl_2$, $AlCl_3 \cdot 6H_2O$ and 11,6 mg of NaCl were added in 600 ppm silicate solution separately. All the experiments with metal ions were performed at 25 °C, and pH was set to 7.

The metal-added SiO_2 solution was taken and completed with ultra-pure water up to 10 mL. The molybdenum yellow spectrophotometry method also measured dissolved silica concentration including metal ions. After 1 mL of the sample solution is transferred to 10 mL as the capacity of the UV-spectroscopy measurement holder, it is poured into a constant volume with distilled water, addition with 500 µL ammonium molybdate and 500 µL sulfuric acid was added. After mixing for 10 min and standing still for 1 min, approximately in an absorption cell, absorbance was measured with a spectrophotometer tuned to wavelength 452. Calibration curves were adjusted to 20 ppm, 40 ppm, 60 ppm, 80 ppm, and 100 ppm.

3.4. Batch Experiment with Tuzla Geothermal Brine

Brine water was taken from Tuzla Geothermal Brine in Ayvacık, Çanakkale. Silica polymerization was also examined in this solution that contains various ions except for SiO_2. The ionic content of the Tuzla brine is shown in Table 3.1.

Table 3. 1 Characteristics of Tuzla brine [58]

Cations	Concentration (mg/L)	Anions	Concentration (mg/L)
Li^+	23.98	**HCO_3^-**	132.19
Na^+	16602.50	**Cl^-**	35170
K^+	1608.40	**F^-**	4.05
Ca^{2+}	2768.59	**NO_3^-**	4.64
Mg^{2+}	114.96	**SO_4^{2-}**	205.43
NH_4^+	105.19	**PO_4^{3-}**	N.D.
pH		6.71	
EC (mS/cm)		83.4	
Salinity (ppt)		58.6	
TDS (mg/L)		62000	
Total alkalinity (mg/L as $CaCO_3$)		108.36	
B (mg/L)		24.56	
As (µg/L)		37.11	
SiO_2 (mg/L)		230	

SiO_2 concentration in brine water is around 180 ppm, which is high enough to follow the polymerization. Since the solution is geothermal brine in this part of the experiment, it was possible to suggest a method to reduce or prevent scaling problems in Tuzla geothermal power plant. Like the batch experiment with synthetic solution, brine water was also investigated at different pH and temperatures. To monitor the effect of the temperature of brine water, about 6 h of experiments were performed at 25 °C and 90 °C. For the pH-dependence experiment, pH 5, 7, and 8 were performed at 25 °C. Temperature-dependent results were used to determine the rate and kinetic calculations of the polymerization.

First, one liter of brine water was filtered and taken into a plastic beaker. For each experiment, 150 mL of the filtered solution was used to prevent impurities. After taking out the sample, the pH was set within the shortest time to the desired value. Since the original pH of the brine water was detected as 6.9 before starting the experiment, the pH setting was done just in seconds, and both before and after the initial concentration during the pH set was recorded.

CHAPTER 4

RESULTS AND DISCUSSION

The rate of silica polymerization was studied in various separate batch reaction experiments utilizing 1000 ppm (0.02 M) sodium silicate as an initial solution, where pH varies between 5 and 9. The concentration of molybdate-reactive silica was monitored using spectroscopy to monitor the polymerization process.

4.1. Silica Concentration

4.1.1. Determination of the concentration via spectroscopy

In situ measurement during the polymerization process, every sample was scanned by wavelength in the range of 350–900 nm, just to be sure. Still, the results at 452 nm were used for computations.

As a representative example of any experiment, calibration was performed with HACH standard silica solution with a 1000 mg/L concentration. In Table 4.2, it has been confirmed that the results obtained by wavelength scanning from the spectrophotometer is consistent and will give precise results in the experiment with both synthetic and natural geothermal brine. Since the calibration was repeated before each experiment, the calibration points were changed from 20 mg/L to 100 mg/L. (Fig 4.1) However, the analysis of the solution concentration was started when the calibration curve had given precise results.

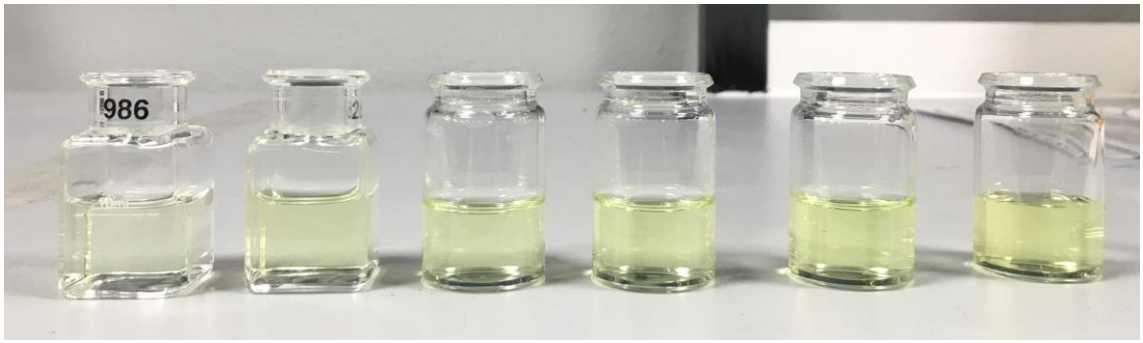

Figure 4. 1. Silicomolybdic samples from 20 mg/L to 100 mg/L.

The example of wavelength and its optical density for all experiments is presented in Table 4.1. The calculation of the concentration of SiO_2 was determined from the calibration curve.

Table 4. 1 Calibration curve at 434 nm and 452 nm wavelength.

	optical density	
concentration (ppm)	**434 nm**	**452 nm**
100	2.57	1.01
50	1.39	0.53
25	0.68	0.26

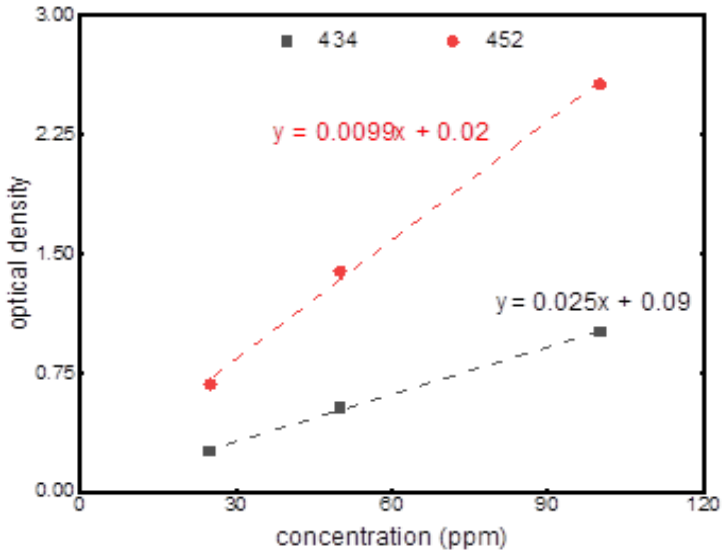

Figure 4. 2. Calibration curve optical density at 434 nm and 452 nm wavelength.

The solution prepared as 600 mg/L of SiO_2 has been designed to construct a calibration curve (Figure 4.2). This estimation of silica concentration based on the calibration curve yields close results to the concentration of the solution prepared for the reliability of the spectroscopic measurement.

Table 4. 2 Calculated concentration (mg/L) from the calibration curve

	434 nm	**452 nm**
Formulas	**0.025x + 0.09**	**0.0099x + 0.02**
HACH solution	52	51.5
Unknown sample	616.4	609.09

4.1.2. Effect of Temperature

The effect of temperature was studied at the temperature range of 25°C (298 K), 45°C (318 K), and 90°C (363 K). The results are shown in Figure 4.3. The concentration of monomeric silica rapidly drops over time at all temperatures and shows exponential decay till the silica solubility at the temperature of interest. The monomeric silica concentration approaches the solubility level for all temperatures in 6 h. Dixit et al. stated that this continuing decreasing lasted for about 3 days for the 25°C experiment.[35] The experiment at 25°C shows the rapid decrease of monomeric silica concentration.

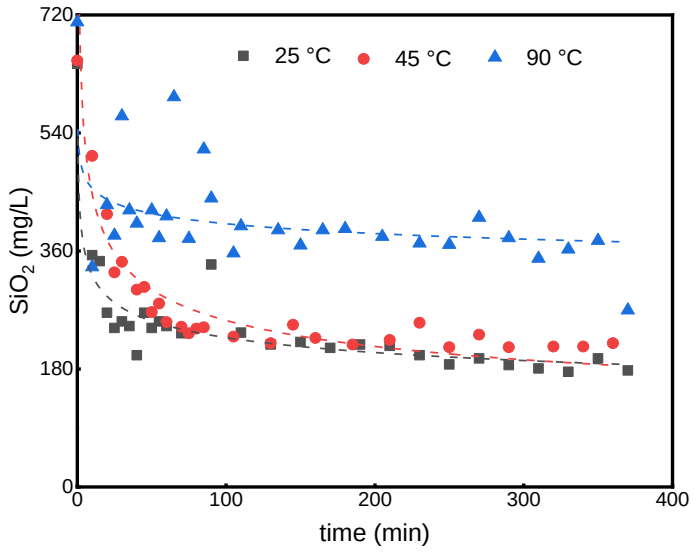

Figure 4. 3. The concentration of dissolved silica at different temperatures at neutral pH.

4.1.3. Effect of Metal Ions

Fig 4.4. shows the concentration of monomeric silica concerning reaction time attained with the same concentration of the metal ions (Fe^{+3}, Al^{+3}, Mg^{+2}, Na^{+}) at 0.01 M. The effect of metal ions is examined at the same reaction conditions to understand the potential impact of the existence of the metal ions on polymerization. Similarly, the concentration of silica shows an exponential decay such that a sharp decrease of the concentration and level off till to the solubility of silica in the presence of the metal ions. Initially, silica is rapidly consumed then the consumption rate is reduced, suggesting that there are not enough silica molecules to keep this rate. The concentration of the silica is not high enough for polymerization. Similar to this mechanism, the results obtained in the presence of metal ions show a similar decrease in silica concentration. The maximum consumption is seen in the presence of Fe^{3+}. The consumption rate is higher than the one of blank, i.e., polymerization without Fe^{3+}. This result may suggest that the consumption is heavily seen since Fe^{3+} is reactive in polymerization. One can speculate that Fe(silicate) may be the initial compound in the formation of the geothermal deposit in the actual geothermal field. Mg and Al also show similar effects on polymerization, triggering the appearance of corresponding metal silicates. Apart from these three ions, Na^{+} shows the opposite behavior. The existence of Na^{+} reduces the rate of consumption of monomeric silica. It may be one of the reasons that Na^{+} is not present in the deposit of the Tuzla geothermal field.

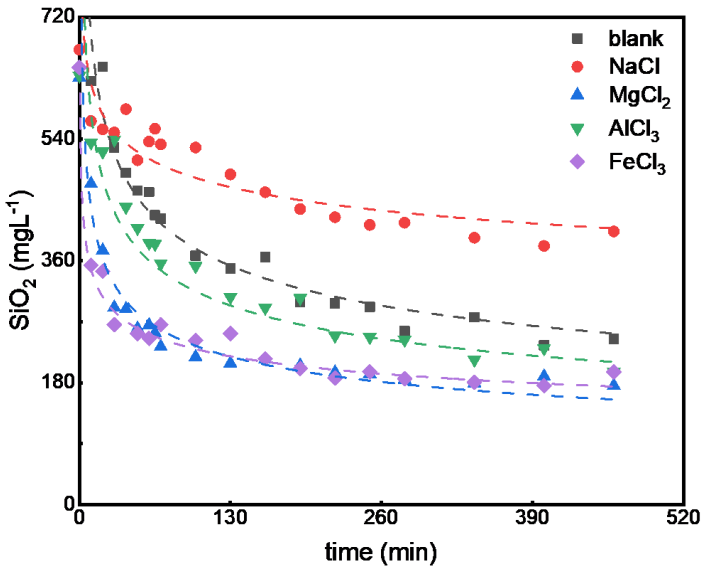

Figure 4. 4. The concentration of dissolved silica.

Complexation between monomeric silica and metallic ions, hydrolysis reaction of silicate ions, and self-polymerization of metal silicates are three types of reactions for the monomeric silica system with metallic ions. Eq. (4.1), Eq. (4.2), and Eq. (4.3) show the reaction formula at pH > 2 and complexation, hydrolysis, and polymerization, respectively. [56,59,60,61]

$$H_4SiO_4 + H_3SiO_4^- \Leftrightarrow H_6Si_2O_7 + OH^- \quad (4.1)$$

$$M^{n+} + H_4SiO_4 \Leftrightarrow M\,OSi(OH)_3^{(n-1)} + H^+ \quad (4.2)$$

$$M^{n+} + n\,H_2O \Leftrightarrow M(OH)_n + nH^+ \quad (4.3)$$

Posterior studies explained these three possible mechanisms of metal effects on silica polymerization. The polymerization mechanism (self-polymerization) of monomeric silica, complexation between monomeric silica and metal ions, and hydrolysis reaction of monomeric silica between metal ions.[13,62] (*M* represents the metal ions and here represents Fe^{+3}, Al^{+3}, Mg^{+2}, Na^+). Xingmei et al. observed the effect on metal ions for polymerization and gelation.[56] When monomeric silica reacts with Fe^{+3} or Al^{+3}, Si-O-Fe (or Al) bonds are formed. The high polymerization rate of Fe^{+3} can be the reason for having a stronger hydrolysis reaction with monomeric silica. [56,59,60,61]

The effect of metal ions on silica polymerization was investigated by adding the ions separately and mixing, keeping the rest of the reaction parameters unchanged. Each metal salt was added to 6oo mg/L silica solution, and the experiment was repeated using the same procedure described above. Concerning Figure 4.4, the SiO_2 concentration shows no significant change at room temperature. (25 °C) It shows the difference in dissolved silica concentration in experiments with and without Fe^{3+}, Al^{3+}, $Mg^{2+,}$ and Na^+. Without adding Fe^{3+}, Al^{3+}, $Mg^{2+,}$ and Na^+ (the ionic strength is the same in both systems, and the pH is adjusted to 7), the silica concentration decreases rapidly after the reaction starts.

Moreover, the experiment was tried at low pH, and there were not remarkable changes in concentration. It had an induction period for both blank and metal ions included solutions. The effect of metal ions on silica polymerization was investigated at different temperatures when the pH of the solution was neutral.

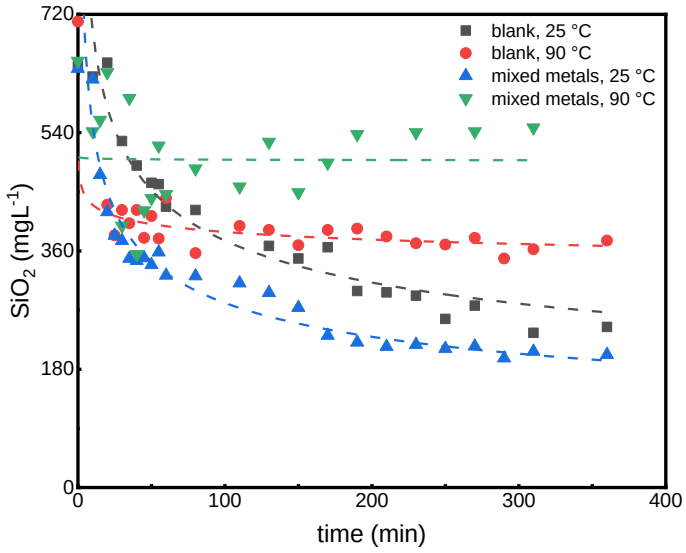

Figure 4. 5. Silica concentration at 25 °C and 90 °C in the absence (blank) and with *mixed* metal ions.

Figure 4.5. shows that the polymerization mechanism has different regimes. When comparing the blank solution and the one with metal ions at 25 °C, the rapid descending of silica concentration shows a similar trend for both. However, one may suggest that the coexistence of the Fe^{3+}, Al^{3+}, $Mg^{2+,}$ and Na^{+} ions may accelerate the polymerization process.

A sharp decrease in concentration was observed for up to 90 min in both solutions. Also, concentration differences (silica consumption) up to 6 h were determined as 397 ppm for the blank sample and 435 ppm for the metal-containing solution. These results may indicate that the dissolved silica concentration is more depleted with metals, which probably causes the formation of metal silicates in the system.

The experiment performed at 90°C did not show rapid and regular decrease except for the data collected in the first 1,5 h. Therefore, the rate of silica consumption for blank and metal-containing samples at 90 °C was compared only in this time interval. Usually, when the temperature gets higher, it is expected that the monosilicic acid and metals interaction should be increased, and accordingly polymerization mechanism is supported with metals. However, even after 1,5 h, the metal, including the solution, gave a nearly similar decreasing trend with the blank one. A conclusive result for the effect of temperature on metal silicate polymerization could not be obtained. Moreover, there is no clear picture in the literature on the tangible impact of metal on the kinetics of the polymerization process at high temperatures.

4.1.4 Effect of pH

It is known that pH has a strong effect on silica polymerization same as temperature. The concentration of molybdate active silica initially contained about 650 mg/L SiO_2. It has been used for the 6 h of polymerization. For the pH range employed in this study, from 5 to 8, the rate of silica polymerization shows remarkable variation. In the initial stages of the experiment, monomeric silica concentrations are relatively stable for some time before starting to decrease. At relatively low pH, the polymerization was found to be slow, and it is considered an induction period in the literature. This time is estimated to be the formation of the crucial size of the polymeric silica network.[18,24] After the induction period, the monomeric silica concentration at pH 5 decreases very slowly, and after 9 h, no equilibrium has been reached. However, the monomeric silica concentration at pH 7 and 8 rapidly decreases without an induction period.

Silica concentration does not show a rapid decrease when the media is acidic (pH=5). The fall of silica concentration was seen but was slower than the results at higher pH. At pH=5, the induction period was about 60 min, but at pH above 7, this induction period is not observed in our experiments. It is known that when the pH is neutral of the solution, the polymerization rate is faster.[13] Figure 4.6 confirms this hypothesis.

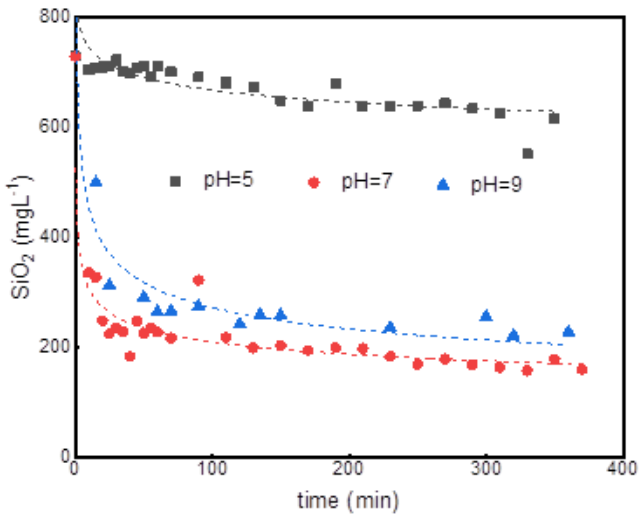

Figure 4. 6. The concentration of monomeric silica at various pH.

A faster SiO_2 concentration decrease means more rapid polymerization. The general pattern shows that at higher pH, monomeric silica concentration is closer to equilibrium regarding amorphous silica after 60 min of polymerization. In conclusion, all investigations indicate that the concentration of monomeric silica decreases over time but after an induction phase at a low pH (pH=5).

Numerous authors observed the induction period reported in the literature with pH value and the degree of supersaturation and temperature. After this induction time, the monomeric SiO_2 concentration decreases towards equilibrium solubility. It should be noted that the induction period may vary from a few minutes to several hours.[9,35,63] Since the initial SiO_2 concentration was about 600 mg/L; it can be concluded that the results are compatible with the results in the literature. [18,40,41,57]

Considering all of these, lowering the pH of the brine can be a remedy to prevent silica scaling in the geothermal system. Lowering pH also causes the dissolution of already-formed metal silicates in the power plants.[1] However, considering the brine is at a higher temperature than the experimental conditions (25 °C), in principle, at this lower pH, it takes a long time to prevent silica scale formation.

4.1.5. Rate Order and Activation Energy

Rate order and activation energy for the silica polymerization in the absence and presence of metal ions is examined for both synthetic and natural brine. The rate of the experiments was calculated for 25°C, 45°C, and at neutral pH. Since the polymerization mechanism has no direct linear decrease, the decreasing function has divided into two regimes. (Figure 4.7a) Moreover, determining the reaction order is complicated because of the induction period during which little or no observed polymerization occurs. However, the temperature experiment has not been observed during the induction period. The first regime is the first 40 min, and the second one is from 40 min to 360 min and from the initial to the end of the experiment duration.

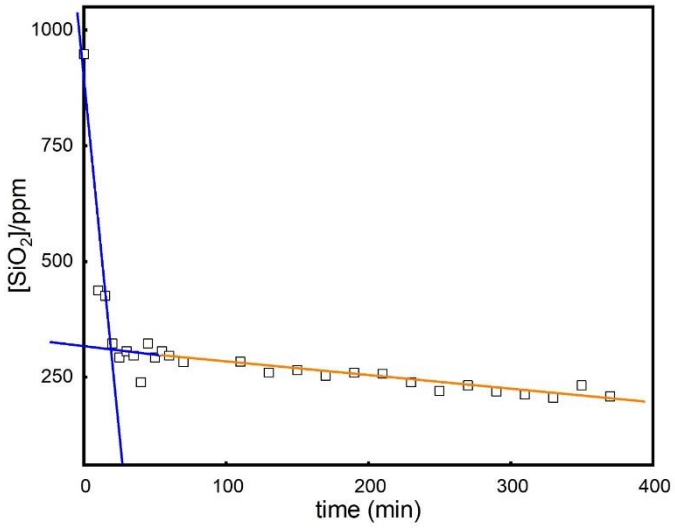

(a)

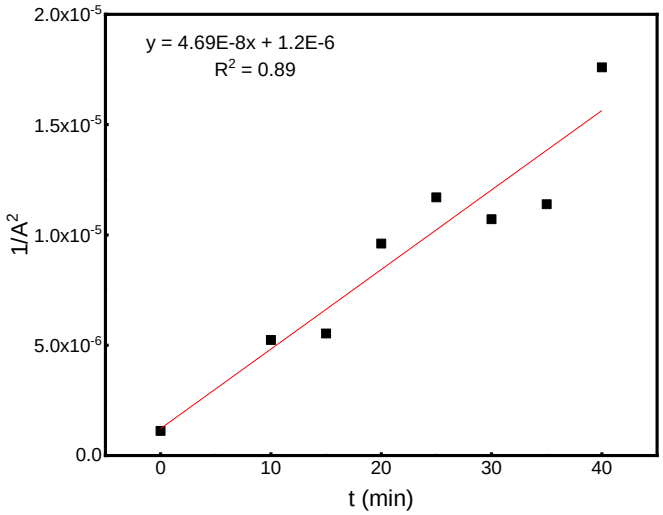

(b)

Figure 4. 7. a) represent the separated part of the function utilized for the estimation of rate order: first 40 min and between 40-360 min b) an example of rate order calculation between time from 0 to 40 min for third order, $1/A^2$ (A represents the concentration of monomeric silica)

Rate constants were calculated from Figure 4.7b for each temperature. The order of the reactions was tested from zeroth to fourth with their R^2 values. The third order rate constant was found most suitable with its 0.91, 0.94, and 0.73 R^2 values for the first 40 minutes, from 40 to 360 minutes and overall, respectively, shown in Table 4.3. While comparing the rate constants of the changing temperature values, the rate constants of the

first 40 min were compared. Thus, the hypothesis that the rate constant increases with temperature was confirmed.

Table 4. 3. The rate constant of silica polymerization at different temperatures and neutral pH (without metals).

T (°C)	Duration (min)	$k_3 \times 10^{-8}$ $(mol/L)^{-2}s^{-1}$	R^2
25	0-40	4	0.91
	40-360	3	0.9
	0-360	4	0.78
45	0-40	20	0.94
	40-360	2	0.58
	0-360	100	0.50
90	0-40	50	0.73
	40-360	0.6	0.68
	0-360	1	0.44

The rate order and the activation energy were calculated for the experiment with metal ions at 25°C, 45°C, and 90°C. It was found that the rate constant increases as the temperature increases. As a general rule in reaction kinetics, temperature accelerates the movement of all molecules such that the number of conspiracy increases and increases the energy of the molecules. All three reactions described above (complexation, hydrolysis, and condensation) continue at a higher rate. At low temperatures, the rate of silica polymerization is typically slow, as the formation of Si-O bonds is an energetically unfavorable process. This means that higher temperatures generally lead to faster polymerization of silica.

Table 4. 4. The rate constant of silica polymerization at 25 °C and 90 °C and neutral pH (with metals).

T (°C)	Duration (min)	$k_3 \times 10^{-8}$ $(mol/L)^{-2}s^{-1}$	R^2
25	0-40	2	0.95
	40-360	6	0.92
	0-360	7	0.95
90	0-40	10	0.8

Table 4.4 presents the rate orders with the existence of metal ions. The rate orders for the 90 °C experiment, except for the first 40 min, are hard to conclude. Between the rate orders for 25°C and 90°C, **only** the first 40 min results will be considered. The increase in temperature seems to be for the first 40 min. When the rate constants of the first 40 min of the experiments performed in the absence and presence of metal were compared, it was seen that the values at 25°C were 4 and 2, respectively. According to Table 4.5, the majority of metal ions have accelerated polymerization. While the catalyst increased the rate, the inhibitor decreased the rate. Higher rate order for Mg^{+2} an Fe^{+3} proves this catalyst increases the reaction rate. Table 4.5 suggests that Na^{+} inhibits the reaction; the rate order is expected to be minimum.

Table 4. 5. The rate constant of silica polymerization at 25 °C with various metal ions at neutral pH.

T (°C)	**Duration (min)**	**$k_3 \times 10^{-8}$ $(mol/L)^{-2}s^{-1}$**	**R^2**
Fe^{+3}	0-40	30	0.9
	40-360	4	0.92
	0-360	5	0.8
Mg^{+2}	0-40	30	0.95
	40-360	6	0.93
	0-360	8	0.87
Na^{+}	0-40	2	0.6
	40-360	1	0.95
	0-360	1	0.95
Al^{+3}	0-40	5	0.76
	40-360	5	0.97
	0-360	5	0.97
blank	0-40	5	0.87
	40-360	4	0.94
	0-360	200	0.93

To get further insight into the entire reaction, the reaction time is divided into two intervals: the first 40 min and the rest of the reaction till 360 min. In the first interval, the response goes faster. Since there are a high amount of unreacted monomeric silica species, the polymerization goes fast. After the first interval is over, the amount of monomeric silica

species is depleted, there is not enough amount of monomer to carry out the polymerization, so the concentration decreases slowly and levels off at the solubility border. While the results at 25°C have the highest R^2 value, at 45°C and 90°C have lower R^2 values. The fitting at low temperatures seems more reliable in this sense.

The activation energies between 25 to 45°C and 25 to 90°C for the overall experiment were determined as 26 ± 1.19 kJ/mol and 27.4 ± 2.98 kJ/mol, respectively. (Table 4.6.) For the first 40 min, the activation energies between 25 to 45°C and 25 to 90°C were determined as 29.52 ± 2.28 kJ/mol. And 27.4 ± 2.98 kJ/mol, respectively. (Table 4.7.) Comparing the literature, this study's result has lower activation energies. Dixit et al. found 52 kJ/mol for the Bouillante geothermal brine with an initial SiO_2 concentration of about 600 at neutral pH.[40] Rothbaum and Rohde found that the activation energy between 5 and 90°C has a low value of 12.25 kJ/mol, while the activation energy between 90 and 180°C appears negative.[41] After the induction period, they observed the maximum rate order for monomeric silica has fourth-order dependence between 5 and 90°C. Carroll et al. found the activation energy as 61 ± 1 kJ/mol for Wairakei geothermal brine between 80 and 120°C at about neutral pH. Also, for higher temperature ranges (20°C to 500°C), the activation energy was observed between 30 to 150 kJ/mol. The reason for the differences between the literature and this study may be the initial solutions, the experimental conditions, and the calculation methods.

Table 4. 6. The activation energies of silica polymerization at different temperatures and neutral pH (without metals)

Overall		
T (°C)	**E_a (kJ·mol^{-1})**	**R^2**
25 - 45	26 ± 1.19	0.94
25 – 90	27.4 ± 2.98	0.98

Table 4. 7. The activation energies of silica polymerization at different temperatures and neutral pH (without metals)

First 40 min		
T (°C)	**E_a (kJ·mol^{-1})**	**R^2**
25 - 45	29.52 ± 2.28	0.94
25 – 90	30.2 ± 2.98	0.98

4.1.6 Experiments with Tuzla brine

The results show no huge differences because of the initial concentration, as seen in the synthetic silica solution. The initial engagement was 181 mg/L as SiO_2, and the induction period was observed when the solution was heated to 90 °C. Generally, the induction period was kept at a high temperature for about 2-3 h from starting the polymerization. However, in Tuzla brine, the induction period has not been observed.

According to Figure 4.8, when the effect of pH at 25 °C in Tuzla brine is examined, the effects easily seen in the synthetic solution are not observed. The most important reason for this should be the higher initial concentration than synthetic brine. The initial silica concentration of the studied Tuzla brine is very close to the equilibrium concentration (180 mg/L for silica) at the pH currently studied. Considering that the state where the polymerization mechanism proceeds the fastest is the region from the high concentration to the equilibrium concentration, polymerization is not observed at this concentration. When the initial concentration is almost at a state of equilibrium concerning amorphous silica, an induction phase is seen during which the molybdate yellow technique shows little or no polymerization.[41]

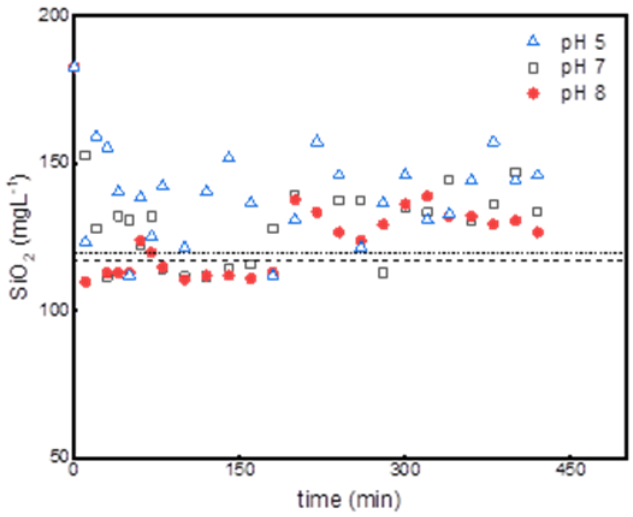

Figure 4. 8. Silica concentration at various pH for Tuzla geothermal brine. Dashed lines correspond to the solubility of amorphous silica at the 25 °C according to Dixit et al. [40]

Figure 4.8 shows the change in dissolved silica concentration for Tuzla geothermal brine. Since the Tuzla brine has a concentration near amorphous silica solubility, the concentration change was limited. Silica in concentration varies between 120 and 180 mg/L. The difference in the concentration of monomeric silica ran in a shallow range between 120 mg/L to 180 mg/L. Since the initial attention was close to the solubility, the concentration did not change exponentially.

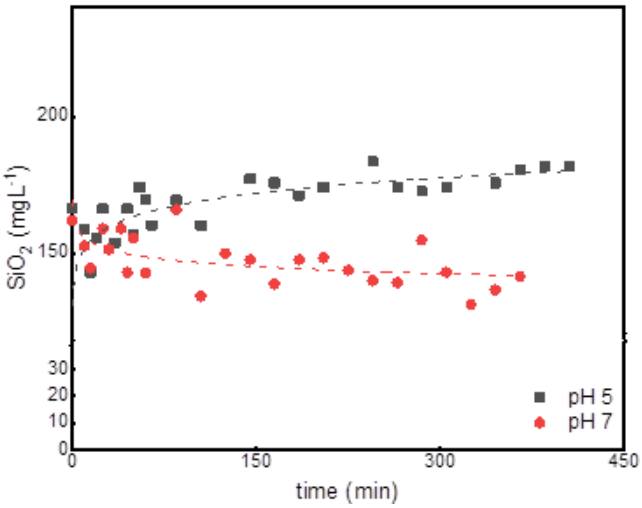

Figure 4. 9. Monomeric silica concentration at pH 5 and 7 at 90 °C for Tuzla geothermal brine.

Figure 4.9. shows that the range of concentration at 90 °C was observed and that the concentration change was not different from the results at 25 °C. Although there are slight changes in the concentration, there is no difference, even as much as 25 °C, as it is still below the equilibrium concentration. According to Dixit et al., a silica equilibrium concentration of approximately 350 mg/L at pH 7 has been calculated between 320 - 340 mg/L at pH 5 and between 360 and 380 mg/L at pH 8. [40] Therefore, as the Tuzla brine concentration is approximately 180 mg/L, it is not surprising that polymerization is not observed.

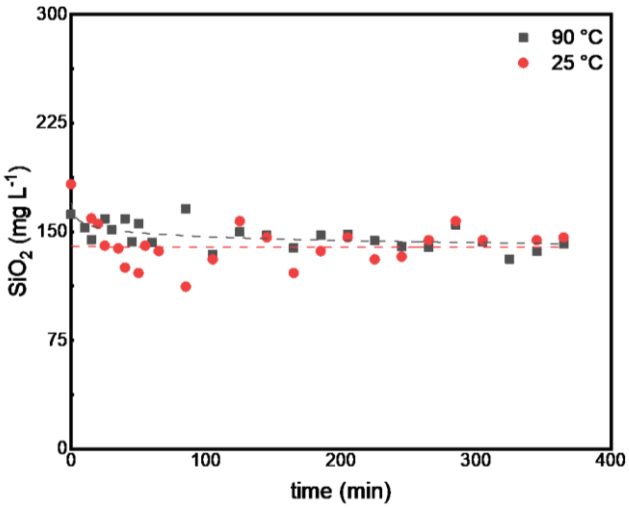

Figure 4. 10. Monomeric silica concentration at 25°C and 90°C at neutral pH for Tuzla geothermal brine.

Figure 4.10 presents the concentration of monomeric silica as a function of reaction time. It shows similar exponential decay for different reaction times at 25°C and 90°C in neutral pH. The consumed silica seems higher at 25°C, from 180 mg/L to a solubility limit of 130 mg/L. However, this change in silica concentration is lower at 90°C from 180 mg/L to 150 mg/L. This is also an expected result since the solubility of silica is higher at high temperatures.

CHAPTER 5

CONCLUSIONS

This thesis aimed to investigate the kinetics of silica polymerization and how the process changes it in the presence of metal ions under various temperatures and pH. The initial concentration of precursor silica is 1 g/L for SiO_2 synthetic solution. All experiments were performed for 6 h reaching the equilibrium of silica concentration. The monomeric silica concentration decreased rapidly in the first 40 min. The initial concentration decreased almost half, even in the first 1 h. Then the concentration slowed down, approaching the solubility of amorphous silica. The polymerization rate was calculated separately for the first 40 min and 40-360 min reaction time.

The rate constant was calculated as 4×10^{-8} for 25 °C, 2×10^{-7} for 45 °C and 1×10^{-7} for 90 °C. The activation energy was 29.52 ± 2.28 $kJ\cdot mol^{-1}$ between 25 °C and 45 °C,and 30.2 ± 2.98 $kJ\cdot mol^{-1}$ between 25 °C and 90 °C. Experiments were conducted at 25°C at pH 5, 7, and 9. It was observed that the optimum condition for the occurrence of silica polymerization was neutral (pH 7). The acidic conditions prevented to decrease in the concentration of monomeric silica. The induction period was only observed at the beginning of the experiments under acidic media, most probably solubility is higher at low pH. It may suggest using acidic inhibitors for geothermal power plants to prevent silica scaling. Fe^{3+}, Al^{3+}, Mg^{2+}, and Na^{+} metal salts were added to the initial solution containing 0.6 g/L of SiO_2 solution. The results suggest that the addition of metal salts except Na^{+} facilitates the polymerization process. The effect of metal salts on silica polymerization was found in $Fe^{3+} \approx Mg^{2+} > Al^{3+} >$ blank $> Na^{+,}$ respectively. Both Fe^{3+} and Mg^{2+} may catalyze the polymerization of silica, which are two main cations in natural geothermal deposits observed in the Tuzla geothermal field.

REFERENCES

(1) Demir, M. M.; Baba, A.; Atilla, V.; Inanli, M. Types of the Scaling in Hyper Saline Geothermal System in Northwest Turkey. *Geothermics* **2014**, *50*, 1–9. https://doi.org/10.1016/j.geothermics.2013.08.003.

(2) Chan, S. H.; Wisconsin, U. S. A. Solubility and Polymerization of Silica. **1989**, *18* (1), 49–56.

(3) Brown, K. Thermodynamics and Kinetics of Silica Scaling. *Proc. Int. Work. Miner. Scaling 2011* **2011**, No. May, 1–9. https://doi.org/10.1002/jcc.21990.

(4) Inanli, M.; Atilla, V. Metal Silicate Formation at Tuzla Geothermal Brine Lines. *Proc. Int. Work. Miner. Scaling* **2011**, No. 2, 25–27.

(5) Baba, A.; Tonkul, S. Conceptual Model for the Tuzla Geothermal Site. **2020**.

(6) Newton, R. C.; Manning, C. E. Quartz Solubility in H2O-NaCl and H2O-CO2 Solutions at Deep Crust-Upper Mantle Pressures and Temperatures: 2-15 Kbar and 500-900°C. *Geochim. Cosmochim. Acta* **2000**, *64* (17), 2993–3005. https://doi.org/10.1016/S0016-7037(00)00402-6.

(7) Karamanderesi, İ. Hydrothermal Alteration in Well Tuzla T-2, Çanakkale, Turkey .PDF. *Geotherm. Train. Program. Reykjavik, Icel.* **1986**, *3*.

(8) Alexander, G. B. The Polymerization of Monosilicic Acid. *J. Am. Chem. Soc.* **1954**, *76* (8), 2094–2096. https://doi.org/10.1021/ja01637a017.

(9) Rothbaum, H. P.; Rohde, A. G. Kinetics of Silica Polymerization and Deposition from Dilute Solutions between 5 and 180°C. *J. Colloid Interface Sci.* **1979**, *71* (3), 533–559. https://doi.org/10.1016/0021-9797(79)90328-X.

(10) Greenberg, S. A.; Sinclair, D. The Polymerization of Silicic Acid. *J. Phys. Chem.* **1955**, *59* (5), 435–440. https://doi.org/10.1021/j150527a014.

(11) Kitahara, S. The Polymerization of Silicic Acid Obtained by The Hydrothermal Treatment of Quartz and The Solubility of Amorphous Silica. **1960**, 131–137.

(12) Reviewed, P.; Berkeley, L.; Cancer, B. Lawrence Berkeley National Laboratory Lawrence Berkeley National Laboratory. **2010**, No. July, 35–43.

(13) Iler, R. K. *The Chemistry of Silica : Solubility, Polymerization, Colloid and Surface Properties, and Biochemistry*; Wiley, 1979.

(14) Choppin, G. R.; Pathak, P.; Thakur, P. Polymerization and Complexation Behavior of Silicic Acid: A Review. *Main Gr. Met. Chem.* **2008**, *31* (1–2), 53–71. https://doi.org/10.1515/MGMC.2008.31.1-2.53.

(15) Jurd, B.; Nolde, J.; Curreri, D. Synthetic Amorphous Silica Product Stewardship. **2011**, 1–5.

(16) European Comission. *Synthethic Amorphous Silicon Dioxide, Scientific and Policy Reports*; 2016. https://doi.org/10.1007/978-1-4020-3995-9_644.

(17) ECETOC. Synthetic Amorphous Silica (CAS No. 7631-86-9). *Brochure* **2006**, No. 7631, 237.

(18) Icopini, G. A.; Brantley, S. L.; Heaney, P. J. Kinetics of Silica Oligomerization and Nanocolloid Formation as a Function of PH and Ionic Strength at 25°C. *Geochim. Cosmochim. Acta* **2005**, *69* (2), 293–303. https://doi.org/10.1016/j.gca.2004.06.038.

(19) Critical Factors Critical Factors for Determining Silica Colorimetric Method. No. 144, 69–80.

(20) Khan, A.; Umar, R.; Khan, H. H. Significance of Silica in Identifying the Processes Affecting Groundwater Chemistry in Parts of Kali Watershed, Central Ganga Plain, India. *Appl. Water Sci.* **2015**, *5* (1), 65–72. https://doi.org/10.1007/s13201-014-0164-z.

(21) Ning, R. Y. Reactive Silica in Natural Waters -A Review. *Desalin. Water Treat.* **2010**, *21* (1–3), 79–86. https://doi.org/10.5004/dwt.2010.1229.

(22) Hauksdóttir, A. Geothermal Energy : Silica Precipitation and Utilization. **2016**.

(23) Gunnarsson, I.; Arnórsson, S. Treatment of Geothermal Waste Water to Prevent Silica Scaling; 2005.

(24) Gunnarsson, I.; Ívarsson, G.; Sigfússon, B.; Thrastarson, E. Ö.; Gíslason, G.; Station, N. P. Reducing Silica Deposition Potential in Waste Waters from Nesjavellir and Hellisheiði Power Plants , Iceland. **2010**, No. April, 25–29.

(25) Wang, W.; Wei, H. Z.; Jiang, S. Y.; Tan, H. B.; Eastoe, C. J.; Williams-Jones, A. E.; Hohl, S. V.; Wu, H. P. The Origin of Rare Alkali Metals in Geothermal Fluids of Southern Tibet, China: A Silicon Isotope Perspective. *Sci. Rep.* **2019**, *9* (1), 1–11. https://doi.org/10.1038/s41598-019-44249-5.

(26) Gallup, D. L. Investigations of Organic Inhibitors for Silica Scale Control in Geothermal Brines. *Geothermics* **2002**, *31* (4), 415–430. https://doi.org/10.1016/S0375-6505(02)00004-4.

(27) Dental X-Ray Diagnostic Device Acidifiction Of Steam Condensate For Incompatibility

Control During Mixing With. 4523279.

(28) Controlled Silica Precipitation in Geothermal. **1989**, *18* (1), 105–112.

(29) Ueda, A.; Kato, K.; Mogi, K.; Mroczek, E.; Thain, I. A. Silica Removal from Mokai, New Zealand, Geothermal Brine by Treatment with Lime and a Cationic Precipitant. *Geothermics* **2003**, *32* (1), 47–61. https://doi.org/10.1016/S0375-6505(02)00050-0.

(30) Veda, I.; Kato, K.; Abe, K.; Furdkawa, T.; Mogi, K. Recovery of Silica from the Sumikawa Geothermal Fluids by Addition. **2000**.

(31) Sinclair, L. A. *DEVELOPMENT OF A SILICA SCALING TEST RIG*; 2012.

(32) Gorrepati, E. A.; Wongthahan, P.; Raha, S.; Fogler, H. S. Silica Precipitation in Acidic Solutions: Mechanism, PH Effect, and Salt Effect. *Langmuir* **2010**, *26* (13), 10467–10474. https://doi.org/10.1021/la904685x.

(33) Kley, M.; Kempter, A.; Boyko, V.; Huber, K. Mechanistic Studies of Silica Polymerization from Supersaturated Aqueous Solutions by Means of Time-Resolved Light Scattering. *Langmuir*. 2014, pp 12664–12674. https://doi.org/10.1021/la502730y.

(34) Kokhanenko, P. *Hydrodynamics and Chemistry of Silica Scale Formation in Hydrogeothermal Systems*.

(35) Dixit, C.; Bernard, M. L.; Sanjuan, B.; André, L.; Gaspard, S. Experimental Study on the Kinetics of Silica Polymerization during Cooling of the Bouillante Geothermal Fluid (Guadeloupe, French West Indies). *Chem. Geol.* **2016**, *442*, 97–112. https://doi.org/10.1016/j.chemgeo.2016.08.031.

(36) Latour, I.; Miranda, R.; Blanco, A. Silica Removal with Sparingly Soluble Magnesium Compounds. Part II. *Sep. Purif. Technol.* **2015**, *149* (July), 331–338. https://doi.org/10.1016/j.seppur.2015.05.037.

(37) Latour, I.; Miranda, R.; Blanco, A. Optimization of Silica Removal with Magnesium Chloride in Papermaking Effluents: Mechanistic and Kinetic Studies. *Environ. Sci. Pollut. Res.* **2016**, *23* (4), 3707–3717. https://doi.org/10.1007/s11356-015-5542-z.

(38) Carroll, S.; Mroczek, E.; Alai, M.; Ebert, M. Amorphous Silica Precipitation (60 to 120°C): Comparison of Laboratory and Field Rates. *Geochim. Cosmochim. Acta* **1998**, *62* (8), 1379–1396. https://doi.org/10.1016/S0016-7037(98)00052-0.

(39) Setiawan, F. A.; Rahayuningsih, E.; Petrus, H. T. B. M.; Nurpratama, M. I.; Perdana, I. Kinetics of Silica Precipitation in Geothermal Brine with Seeds Addition: Minimizing Silica Scaling in a Cold Re-Injection System. *Geotherm. Energy* **2019**, *7* (1).

https://doi.org/10.1186/s40517-019-0138-3.

(40) Dixit, C.; Bernard, M. L.; Sanjuan, B.; André, L.; Gaspard, S. Experimental Study on the Kinetics of Silica Polymerization during Cooling of the Bouillante Geothermal Fluid (Guadeloupe, French West Indies). *Chem. Geol.* **2016**, *442*, 97–112. https://doi.org/10.1016/j.chemgeo.2016.08.031.

(41) Rothbaum, H. P.; Rohde, A. G. Kinetics of Silica Polymerization and Deposition from Dilute Solutions between 5 and 180°C; 1979.

(42) Conrad, C. F.; Icopini, G. A.; Yasuhara, H.; Bandstra, J. Z.; Brantley, S. L.; Heaney, P. J. Modeling the Kinetics of Silica Nanocolloid Formation and Precipitation in Geologically Relevant Aqueous Solutions. *Geochim. Cosmochim. Acta* **2007**, *71* (3), 531–542. https://doi.org/10.1016/j.gca.2006.10.001.

(43) Thornton, S. D.; Radke, C. J. Dissolution and Condensation Kinetics of Silica in Alkaline Solution. *SPE Reserv. Eng. (Society Pet. Eng.* **1988**, *3* (2), 743–752. https://doi.org/10.2118/13601-PA.

(44) Al-mutaz, I. S.; Al-anezi, I. A. Silica Reduction in Reverse Osmosis Desalting Plants. *Engineering* **2002**, *2* (December), 3–14.

(45) Sheikholeslami, R.; Al-Mutaz, I. S.; Koo, T.; Young, A. Pretreatment and the Effect of Cations and Anions on Prevention of Silica Fouling. *Desalination* **2001**, *139* (1–3), 83–95. https://doi.org/10.1016/S0011-9164(01)00297-1.

(46) Manno, B. R.; Abukhalaf, I. K.; Manno, J. E. *A Simple Spectrophotometric Assay for the Measurement of Soluble Silica in Water*; 1997; Vol. 21. https://academic.oup.com/jat/article/21/6/503/735411.

(47) Garrett, H. E.; Walker, A. J. The Spectrophotometric Determination of Silicic Acid in Dilute Solution. *Analyst* **1964**, *89* (1063), 642–650. https://doi.org/10.1039/AN9648900642.

(48) Strickland, J. D. H. The Preparation and Properties of Silicomolybdic Acid. III. The Combination of Silicate and Molybdate. *J. Am. Chem. Soc.* **1952**, *74* (4), 872–876. https://doi.org/10.1021/ja01124a004.

(49) Mullin, J. B.; Riley, J. P. The Colorimetric Determination of Silicate with Special Reference to Sea and Natural Waters. *Anal. Chim. Acta* **1955**, *12* (C), 162–176. https://doi.org/10.1016/S0003-2670(00)87825-3.

(50) Studies in the Determination of Silica.Pdf.

(51) Hermosilla, D.; Ordóñez, R.; Blanco, L.; de la Fuente, E.; Blanco, Á. PH and Particle

Structure Effects on Silica Removal by Coagulation. *Chem. Eng. Technol.* **2012**, *35* (9), 1632–1640. https://doi.org/10.1002/ceat.201100527.

(52) Salvador Cob, S.; Hofs, B.; Maffezzoni, C.; Adamus, J.; Siegers, W. G.; Cornelissen, E. R.; Genceli Güner, F. E.; Witkamp, G. J. Silica Removal to Prevent Silica Scaling in Reverse Osmosis Membranes. *Desalination* **2014**, *344*, 137–143. https://doi.org/10.1016/j.desal.2014.03.020.

(53) Latour, I.; Miranda, R.; Blanco, A. Silica Removal with Sparingly Soluble Magnesium Compounds. Part I. *Sep. Purif. Technol.* **2014**, *138*, 210–218. https://doi.org/10.1016/j.seppur.2014.10.016.

(54) Sparks, D. L. Kinetics of Soil Chemical Processes. *Environ. Soil Chem.* **2003**, 207–244. https://doi.org/10.1016/b978-012656446-4/50007-4.

(55) Alshehawy, A. M.; Mansour, D. E. A.; Ghali, M.; Lehtonen, M.; Darwish, M. M. F. Photoluminescence Spectroscopy Measurements for Effective Condition Assessment of Transformer Insulating Oil. *Processes* **2021**, *9* (5). https://doi.org/10.3390/pr9050732.

(56) Shen, X.; Ge, J.; Wang, P.; Wu, X.; Li, L. Polymerization Behavior of Silicic Acid with Fe3+, Al3+, and Ca2+ Coexisting Ions. *J. Sol-Gel Sci. Technol.* **2018**, *85* (2), 480–485. https://doi.org/10.1007/s10971-017-4558-x.

(57) Ishii, S.; Tajima, S.; Takaya, Y.; Fuchida, S.; Tokoro, C. Kinetic Evaluation of PH and Temperature Effects on Silica Polymerization in the Presence of Mg, Al and Fe. *Kagaku Kogaku Ronbunshu* **2021**, *47* (6), 237–244. https://doi.org/10.1252/kakoronbunshu.47.237.

(58) Recepoğlu, Y. K.; Kabay, N.; Ipek, I. Y.; Arda, M.; Yüksel, M.; Yoshizuka, K.; Nishihama, S. Packed Bed Column Dynamic Study for Boron Removal from Geothermal Brine by a Chelating Fiber and Breakthrough Curve Analysis by Using Mathematical Models. *Desalination* **2018**, *437* (February), 1–6. https://doi.org/10.1016/j.desal.2018.02.022.

(59) Exley, C.; Schneider, C.; Doucet, F. J. *The Reaction of Aluminium with Silicic Acid in Acidic Solution: An Important Mechanism in Controlling the Biological Availability of Aluminium?* www.elsevier.com/locate/ccr.

(60) Aramaki, Y.; Yokoyama, T.; Okaue, Y.; Watanabe, K. Chemical Adsorption of Silicic Acid to Aluminum Combined with Cation Exchange and Chelate Resins as Model Compounds of the Surface of Microbes. *Chem. Geol.* **2004**, *212* (3-4 SPEC.ISS.), 339–349. https://doi.org/10.1016/j.chemgeo.2004.08.023.

(61) Swedlund, P. Webster, J., G. ADSORPTION AND POLYMERISATION OF SILICIC ACID ON FERRIHYDRITE, AND ITS EFFECT ON ARSENIC ADSORPTION. *Water*

Res. **1999**, *33*, 3413–3422. https://doi.org/10.1016/s0043.

(62) Brinker, C. J. *HYDROLYSIS AND CONDENSATION OF SILICATES: EFFECTS ON STRUCTURE*; 1988; Vol. 100.

(63) Angcoy, E. C.; Arnórsson, S. An Experiment on Monomeric and Polymeric Silica Precipitation Rates from Supersaturated Solutions. *World Geotherm. Congr.* **2010**, No. April, 25–29.

(58) Tikhomirova, T. I., Krokhin, O. V., Dubovik, D. B., Ivanov, A. V., & Shpigun, O. A. (2002). Journal of Analytical Chemistry, 57(1), 18–23. https://doi.org/10.1023/a:1013649405881

(59) Siever, R. (1962) Silica solubility, 0-200 ° C, and the diagenesis of siliceous sediments. 3. Geol. 20, 127-150.

(60) Vallero, D. A. (2010). Environmental Biochemodynamic Processes. Environmental Biotechnology, 99-165. https://doi.org/10.1016/B978-0-12-375089-1.10003-0